PERFORMANCE OF A SELF-CORRELATING SYNCHRONIZATION AND DETECTION SCHEME FOR IR-UWB IN MULTI-USER MULTIPATH ENVIRONMENTS

BY NIRMAL CHANDRASEKARAN

A thesis submitted to the

Graduate School—New Brunswick

Rutgers, the State University of New Jersey

in partial fulfillment of the requirements

for the degree of

Master of Science

Graduate Program in Electrical and Computer Engineering

Written under the direction of

Professor Larry Greenstein

&

Professor Predrag Spasojevic

and approved by

_____

_____

_____

_____

New Brunswick, New Jersey

October, 2007

Abstract of the Thesis

Performance of a Self-Correlating Synchronization and Detection Scheme for IR-UWB in Multi-User Multipath Environments

by NIRMAL CHANDRASEKARAN

Thesis Directors: Professor Larry Greenstein & Professor Predrag Spasojevic

Owing to the very low duty cycle of impulse like ultra wideband signals, timing acquisition with acceptable accuracy and complexity has been a constant topic of research. Most acquisition techniques can be broadly classified under two categories: *Training based algorithms*, which require a specific training sequence at the start of communication and - *Blind Acquisition*, which relies on the correlation between successive data symbols transmitted and cyclostationarity of the transmitted signal. Amidst algorithms which use a clean template or a noiseless reference, a recent class of techniques named 'Timing based on Dirty Templates' (TDT) has been proposed. These algorithms rely on the correlation of two adjacent portions of the noisy received signal. One portion of the noisy received signal acts as a template for the other, thus improving the synchronization speeds and accuracy by making the acquisition independent of training sequences. A novel blind TDT algorithm, which we refer to as *Agrawal Blind Synchronization scheme (ABS)*, was proposed for IR-UWB signals. Based on the design of the time hopping code, significant improvements in acquisition speeds have been demonstrated using the ABS scheme, compared to existing blind acquisition schemes.

The objective of this thesis is to analyze the performance capabilities of the self-correlating ABS scheme in multi-user multipath environments. Adopting the best performing time hopping pattern, we investigate the effect of multiple interferers on absolute timing error,

under various SNR scenarios as well as multiple symbols used for timing acquisition. Link performance is evaluated through bit-error-rate (BER) analysis under various system conditions. Since we use differential methods for timing acquisition as well as symbol detection, significant energy capture can be achieved in a dense multipath scenario due to *self-Raking*. We also propose modifications to conventional differential detectors to avoid *self-Raking* of interfering pulses. As a comparison to differential detectors, the detection performance of an ideal Rake receiver was tested with the ABS scheme. Our results indicate that the timing error performance the ABS scheme and thus the BER performance of the detection phase deteriorate notably with increase in the number of users in the system. The effective number of interferers is the limiting factor in both absolute timing error and BER performance. In differential detection, the effect of interference is so large it dominates over the effect of timing errors. The use of the ABS scheme is advantageous when Rake receivers are used, since timing error has a drastic effect of degrading the BER performance. The improvements of using ABS scheme in multi-user multi-path environments become more prominent in the case of ideal Rake reception, as compared to differential detection.

Acknowledgements

I am deeply indebted to Dr. Larry Greenstein for all his stimulating suggestions, encouragement and guidance during the course of this thesis. I would also like to thank Dr. Predrag Spasojevic for his constant support throughout.

I am obliged to Shishir Agrawal for providing the foundation which motivated me to embark on this thesis work.

I would also like to thank all my family and friends for their support, interest and valuable advice.

Table of Contents

List of Figures

Chapter 1

Introduction

1.1 Ultra Wideband Communication Systems

In recent times, Ultra Wideband (UWB) communications ([1], [2]) has emerged as a promising contender for indoor and short range wireless communications with very attractive features. The Federal Communications committee (FCC) now defines any technology occupying a bandwidth of more than 20% of its center frequency as a UWB system. In order to accommodate the huge bandwidths and to provide the system designers with a variety of sub-bands to choose from, the FCC introduced a spectral mask in the United States over a huge unlicensed bandwidth (3.6 – 10.1 GHz) in 2002, where UWB radios co-exist with conventional RF systems.

UWB communication systems offer distinctive advantages. Unlicensed UWB radios provide immunity from co-existing narrow-band systems due to the low power spectral density of the transmitted signal. The wideband operations further presents the receiver with sufficient protection from multipath fading and multi-user interference. The system is robust to jamming and intercepts as well. Such promising features of UWB systems make it suitable for short-range, very low power military and navigation applications. It can also be applied to home and wireless personal area networks providing much higher data rates as compared to existing wireless protocols.

1.2 Classes of Ultra Wideband Communication Systems

Two existing forms of Ultra Wideband Systems used are *Carrier-based* and *Impulse Radio (IR)* systems [3]. *Carrier based* UWB systems up-convert the baseband data signal to microwave frequencies using a carrier. The 802.15.3 Standards committee considered a carrier-based 2.4GHz

radio as the PHY layer. IR-UWB was the original form of UWB system proposed. Unlike carrier-based techniques, the transmit signal in IR-UWB is a series of baseband pulses of sub-nanosecond width and very low average power. The transmitted sequence of pulses is usually modulated in time or amplitude with a pseudorandom spreading code, unique to each user in the system. Multiple access is achieved by using various pseudorandom spreading codes for different users. In contrast to the carrier-based system, the advantage of this approach is the low cost and complexity of the receiver. Owing to these advantages, the IR-UWB systems [5]-[14] have found interest in military and navigation applications. The complete focus of this thesis will be on IR-based UWB communication system.

1.3 Challenges in IR-UWB Systems

The advantages of UWB systems come at the cost of physical layer issues in the form of (1) channel modeling, (2) antenna design, (3) pulse shaping and (4) timing recovery. Since the indoor wireless channel gives rise to a dense multipath environment, predicting the multipath propagation is very complicated. Several channel models have been proposed and tested for dense multipath situations with UWB transmitters and receivers ([15]-[19]). In addition, antenna and pulse design pose important challenges due to the distortions effects of UWB antennas and need to satisfy spectral mask requirements. Novel ideas [21, 22] have been proposed to measure, analyze and overcome the distortions due to antenna design. The fourth problem mentioned above, timing recovery ([23]-[31]) is the main focus of this thesis, specifically in the context of IR-UWB.

1.4 Intricacies of UWB Timing Recovery

Impulse radio systems support multiple users by a unique time hopping code assigned to each user. The TH code determines the position of the pulses in each frame of the symbol. This system

model can be used to separate different users transmitting different information simultaneously. However, in the presence of multiple users and multipath reflections, acquiring the timing information of the desired received signal and hence start detecting the data symbol transmitted by the desired user is a challenge.

Obtaining high precision in UWB signal timing becomes difficult due to the very low duty cycle and amplitude of the impulses transmitted. This issue is further deteriorated in the presence of multiple users and multipath interference in the system, wherein the desired user signal is corrupted by pulses from other users' signals and components due to the dense multipath indoor channel. The recovery of timing is significant since at the receiver, the amount of energy capture completely depends on the error in the timing information. If the error is large, the receiver doesn't acquire significant energy from the received signal and thus high probability of bit errors is encountered.

Traditional methods proposed in literature for the timing synchronization of received signals are not applicable to UWB signals due to the narrow pulse width and very dense indoor multipath environments. Thus, a variety of acquisition algorithms have been devised to suit the bandwidth and system requirements of UWB systems [23]-[41]. We concentrate on a particular set of algorithms called *Timing using Dirty Templates (TDT)* in this thesis.

1.5 Benefits of TDT Algorithms

TDT algorithms are mainly interesting due to the improved acquisition speed and low complexity solutions. Most conventional timing recovery algorithms for IR-UWB make use of a clean or *noiseless* template for correlation. TDT algorithms exploit the timing information present in the received signal by using one received symbol to act as a template for the other symbols. Thus the template used for correlation is noisy, since it is derived from the received signal. The use of a noisy or *dirty* template eliminates the time consuming process of generating a local template of

the received signal, which involves searches over thousands of bins. Even though the template is corrupted with noise, multipath components as well as multi-user interference (MUI), the acquisition is much faster compared to other blind algorithms because fewer numbers of operations are involved at the receiver. TDT algorithms can be either *data-aided* [39], which use a judiciously chosen training sequence, transmitted before the start of acquisition to first acquire the timing information from the received signal, before the data symbols are transmitted or *blind TDT* [40], which extract the dirty templates from the received data sequence for timing information and rely on the '*peak-picking*' the autocorrelation. The idea behind either is that the autocorrelation between pairs of successive segments of the received signal will always have a peak at the start or end of each symbol. The received signal is auto correlated with the delay of a symbol period. The timing information can thus be obtained by peak-picking the symbol-long autocorrelation product.

We essentially investigate a novel blind TDT algorithm by Agrawal [41], which uses half-symbol-long window for correlation. The *Agrawal Blind Synchronization* (*ABS*) Scheme, as we term it, removes the dependence of the correlation on the polarity of data symbol sequence since the correlation windows contain pulses either the same data symbol or adjacent data symbols, where the time hopping patterns for a particular user are similar. In this case the autocorrelation between the windows is highest only if the pulses in the two windows are all from the same symbol, which occurs only at the start (or end) of each symbol. The timing acquisition is obtained through prudently designed Time Hopping code pattern, the two halves of which are shifted in time by a unique offset. Thus, the code design offset assigned is unique to each user and differentiates the desired user from the interferers. In a single-user environment, it was shown [41] that the proposed algorithm achieves up to four-fold improvements in acquisition speeds for the same signal-to-noise ratios, when compared to the existing blind TDT schemes. The following section describes the details of the proposed scheme.

1.6 Details of the ABS Scheme

The multi-user opportunities of the ABS scheme are considerable, since the time hopping code design provides separation between users by assigning each user a unique offset. To de-correlate, the receiver of a particular receiver has to use the specific code offset unique assigned to it. With a separation of half a chip time between code design offsets, it has been shown [41] that up to (N_C-1) users can be accommodated in the system at the same time, where N_C is the number of chips per frame. In practical indoor wireless networking scenarios, the received signal is distorted by thermal noise, multi-user interference and multipath distortions. Our goal is to determine the performance limitations of the ABS algorithm when used in a multi-user multipath environment.

We exploit the advantages of the ABS algorithm with different approaches to the time hopping code patterns. Keeping the basic code design the same, the position of the transmitted pulses is varied using different time hopping patterns with uniform and random time hops. We identify the best TH design approach and evaluate the timing error performance of the algorithm with multiple interferers in a dense multi-path environment. The receiver structure used in this system model is classical differential detection [42], though we also propose modifications to the existing detection methods. In the presence of timing error, we analytically determine the bit error rate (BER) conditioned on timing error and then average the expressions using the cumulative distributions of timing error obtained through simulations. Finally, the BER vs SNR performance of the algorithm is presented, under a wide variety of system parameters and interference conditions.

1.7 Organization of the Thesis

The main work done in this thesis is motivated by the novel timing acquisition algorithm, we call the ABS scheme. We extend the earlier to analyze the performance of this scheme in a multi-user, multi-path environment. Chapter 2 discusses the multi-user capabilities of the ABS scheme with

different TH code patterns, receiver processing and interference model. Chapter 3 summarizes the timing error performance with multiple interferers and presents the results from simulations. Chapter 4 delineates the detector structure and BER performance of the system in a multi-user, multi-path environment. Chapter 5 summarizes the results, the advantages and disadvantages of the code in a multi-user environment and possible future work.

Chapter 2

Literature Review

2.1 Introduction

Numerous algorithms have been devised to obtain accurate timing information from a received UWB signal. Two main classes of algorithms can be identified: *Training-based* or data aided algorithms which require training sequences to be transmitted before or during the communication, and *blind* or non-data aided algorithms, which use the information bearing data symbols for the timing acquisition. The training sequence for the former techniques may be a specific stream of symbols or a preamble of non-time hopped pulses or a combination of both. This sequence is known by the receiver and is used to acquire the timing of the received signal. Since separate training bits are required, the effective information bit rate is reduced. The blind algorithms are very useful in scenarios of broadcast networks where nodes may join the network at any time, thus a training sequence might be unavailable for the node. The drawback of non-data aided algorithms is that it requires more symbols for precise acquisition which leads to slower synchronization and possibly greater computational complexity. The primary focus of this thesis will be on non-data aided algorithms, but existing acquisition schemes will be explained and compared in the forthcoming sections.

2.2 Data Aided Acquisition Algorithms

Many data aided algorithms are reported in the literature. One of the earliest serial search-based algorithms was proposed in [23]. It involves bit-reversal search within a frame, which enhanced acquisition speeds for an unmodulated set of pulses. The idea behind this strategy is that a linear search will not be optimal for a signal in a dense multipath channel, where various positions inside a frame may have considerable energy for timing acquisition. An improvement has been

suggested by combining bit-reversal scheme with a modified version of double-dwell search [24], utilizing search windows with two step-thresholds for superior acquisition speeds. Both these techniques use a preamble for acquisition, using non-time hopped pulses. Equal gain combining [26] was proposed as the method to collect multi-path energy since the UWB signals traverse through a dense multipath environment with little fading [25]. Several averages of a time shifted symbol templates is used as a signal template to collect the multipath energy and improve accuracy.

A novel listener technique, using Kasami sequences and divide-and-conquer localization algorithms, was proposed to effect rapid acquisitions [27]. This technique applies to time-hopped pulse doublets (two pulses of opposite polarity and separated in time). Another technique to acquire non-time hopped pulses sequences involving the transmission of separate synchronization pulses, for the acquisition stage was devised in [28]. The transmit sequence consists of pulses for information interleaved with pulses for timing acquisition. Once the receiver synchronizes to these pulses for timing, the timing information of the pulses transmitted for information can be acquired directly from their time difference. The aforementioned techniques apply to non-time hopped sequences and have not been used for the newer modulation schemes involving chip-level time-hopping in each frame of the transmitted data symbol.

In more recent developments in signal acquisition for time hopped pulse sequences, a correlator-based acquisition scheme has been suggested in [29]. The method involves finding energy over quantization of the frame time, and correlating them with a scaled version of the pseudo random sequence. Once the peak values of output correlations are calculated, the receiver does a finer search only in those frame positions. This yields coarse chip-level timing information with quite good acquisition speeds. Improvements have been made to this technique, with analysis of the trade-off between performance and the computational requirements of the algorithm [30]. Efficient Maximum-Likelihood (ML) techniques have also been devised for time-hopped as well as non-time-hopped pulse sequences. One such algorithm in the literature [31]

requires a large number of searches even though it is optimal since it uses ML acquisition and does not require sub-nanosecond sampling.

A new class of acquisition schemes, termed as *Differential Detection Acquisition,* makes use of the inherent transmitted delay between pulses to acquire the timing of the received pulses. One such procedure suggested in [32] required the design of a novel time hopping pattern in which the time difference between the transmitted pulses is related to the position of the pulse in the symbol. Thus the timing of the received signal can be acquired by using the time difference between the received pulses. The inability of this scheme to perform in dense multiple access environments, where interfering users clutter the environment with their signals, has been addressed and changes have been made in [33].

An algorithm which attempted for channel estimation and acquisition together was developed in [35]. A preamble of periodic UWB pulses with no time hopping or modulation are transmitted first and utilized to estimate the channel. This is followed by a known symbol sequence. The frame timing and channel estimate acquired from previous step are used to acquire the timing of this data sequence. In contrast, a novel dual spreading pattern (time hopping and direct sequence spreading) was presented in [34], where the transmitted signal is first spread using a time hopping code and then by a direct sequence spreading code. At the receiving end, timing is acquired by square looping to remove the DS spreading first, and acquire the TH sequence. Another stage deals with the DS sequence acquisition. The use of short TH codes drastically improves acquisition speeds during the reception process.

2.3 Blind Acquisition Algorithms

In contrast to training based techniques which utilize coarse chip level search algorithms, the *Non-Data-aided* or *Blind* acquisition techniques make use of the cyclostationarity of the repetitive UWB pulse sequences. The two methods have been thoroughly analyzed and compared in [36].

Several techniques have been proposed which do not require training sequences to be transmitted. One such algorithm proposed in [36] makes use of the frame rate sampled correlator outputs to obtain timing. In two ideas proposed, the received signal can be acquired either by peak picking the frame rate samples of autocorrelation between adjacent symbols or from the phase of cyclic correlation of frame-rate correlator outputs. The correlation is done between the received signal and a template symbol waveform. The need to use multiple symbols (≈100-120) for sufficient accuracy makes this acquisition slower. The algorithm has been thoughtfully modified in [37] where a carefully chosen segment of the received signal is used instead of a template of transmitted symbol waveform, thus utilizing the multipath diversity gains in the received signal. The limitation of both these algorithms is that they can be used only on slow-time hopped UWB signals, wherein the time hopping is from symbol to symbol rather than frame to frame.

2.4 Timing Based on Dirty Templates

Timing using dirty templates (TDT) is a particularly interesting set of acquisitions schemes due to the improved acquisition speed and low complexity solutions. All algorithms described until now make use of a clean or *noiseless* template for correlation. TDT algorithms exploit the timing information present in the received signal by using one received symbol to act as a template for the other symbols. Thus the template used for correlation is noisy, since it is derived from the received signal. The use of a noisy or *dirty* template eliminates the time consuming process of generating a local template of the received signal, which involves searches over thousands of bins. Even though the template is corrupted with noise, multipath components as well as MUI, the acquisition is much faster compared to other blind algorithms because fewer numbers of operations are involved at the receiver. Our focus is on the blind TDT schemes which extract the dirty templates from the received signal, in contrast to data-aided TDT where a judiciously chosen training sequence is transmitted which quickens the acquisition process.

In one of the early developments of blind TDT acquisition of UWB signals, authors of [40] came up with a scheme which utilizes the existing symbol as a dirty template for the next symbol. Two successive symbol long windows are correlated and the process is repeated by sliding the windows N_f times at intervals of N_f, where N_f is the number of frames per symbol. Peak picking the correlation output gives the timing of the frame closest to the start or end of a symbol. Relying on a simple Integrate and dump operation per symbol, the scheme provides a frame level timing acquisition with reduced complexity and markedly improved acquisition speeds.

An alternate blind TDT algorithm devised in [41] uses half-symbol-long windows for correlation, rather than symbol long windows in other existing schemes. Through analysis and simulations, it was shown [41] that the proposed algorithm achieves up to four fold improvements in acquisition speeds for the same signal-to-noise ratio (in a single-user environment), when compared to existing schemes. The study of this scheme under various designs, its performance in a multi-user, multipath environment and the resulting BER curves are the prime focus of this thesis.

Chapter 3

The ABS Scheme – Existing Model and Variations

3.1 Introduction

Timing using dirty templates has been an interesting topic of research owing to simplifications of receiver models, improvements in accuracy and faster acquisition speeds. The ABS scheme delineates a novel blind algorithm using dirty templates, with a unique code design to accommodate up to N_c-1 users, for N_c chips per frame. This is chapter discusses the ABS system model, various modifications to the TH patterns in the code, receiver processing approaches and its applicability to multi-user multipath environments.

3.2 ABS Scheme with Multiple Access

Every symbol is considered to be made of N_f frames, Each frame contains a pulse hopped over the frame by a distance defined by a pseudo-random time hopping sequence, as in Figure 3.1. In this Figure, the pulse is placed in the first chip of the frame for illustration purposes. The frames are made up of N_c chips each and only one of the chips contains the pulse in each frame. In the actual system, the pulse can be time hopped among N_c chips per frame available. The time hopping code is designed in a way that,

$$c_{j+ N_f /2} = c_j + \delta_i \quad 0 \le j < N_f /2 \quad \text{……..(3.1)}$$

δ is the specific code offset of user *i*. The term c_j denotes the time hop code for the j^{th} frame. Thus in each frame of the second half of the symbol, the time hop code $c_{j+ N_f /2}$ is shifted from the corresponding frame in the first half (c_j) by a user specific code offset δ. This unique offset enables each user to synchronize in the presence of other users, as we explain next.

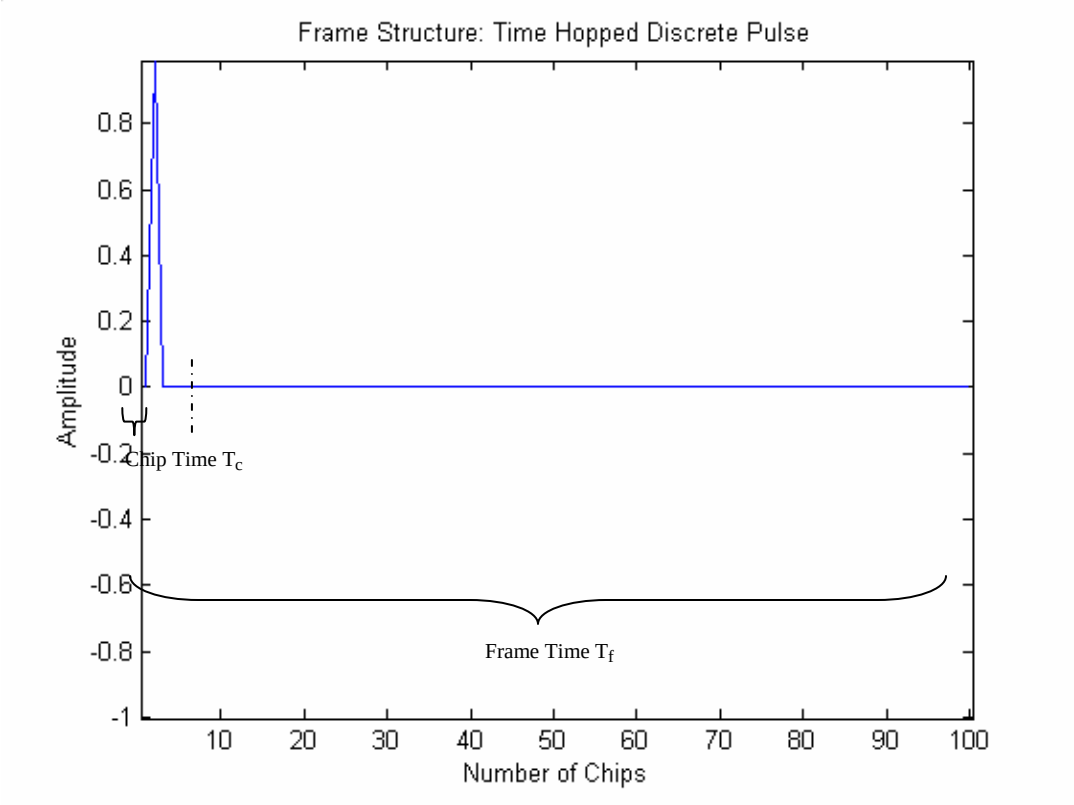

Figure 3.1: Frame Structure of Time Hopped Discrete Pulse

We will describe the algorithm in the presence of multiple users. For the sake of simplicity of this discussion, we again do not take into consideration the effects of multi-path channel and additive Gaussian noise. We will of course, include them in our calculations. Consider the simple case of a single user in the system, as shown in Figure 3.2. We define δ_1 as the code offset of the desired user. So, each symbol of the desired user signal has the same TH pattern in the first half, except that in the second half of each symbol, the pulses are shifted according to (3.1). For illustrative purposes, we have considered $N_f = 6$ frames/symbol and $N_c = 100$ chips per frame. Thus number of pulses per symbol is 6 (Figure 3.2). Note that the amplitude modulation code in the frames repeats every half-symbol, while the TH code pattern repeats every symbol. Let us first assume acquisition starts at the start of the symbol. As depicted by Figure 3.3, at the receiving end, the received signal is first delayed by $N_f/2$, and then by δ_i, so that pulses from the two halves of symbol line up perfectly. The received signal is multiplied with a delayed version of itself and the autocorrelation over half a symbol period is stored for future

comparison. This process is repeated for N_f*N_c starting instances, at intervals of N_c. It is to be noted from Figure 3.3, the product of the received signal with its delayed version yields components only if the pulses belong to the same symbol. Pulses from two different symbols do not line up when the product is evaluated due to the design offset given to the second half of each symbol. The index of the maximum autocorrelation obtained gives the acquired timing of the start of the symbol (Figure 3.4). The accuracy of this acquired timing information can be improved by averaging the autocorrelation over multiple symbols. Adding up autocorrelations in M symbols and then "peak-picking", will result in a reduced timing error as will be demonstrated.

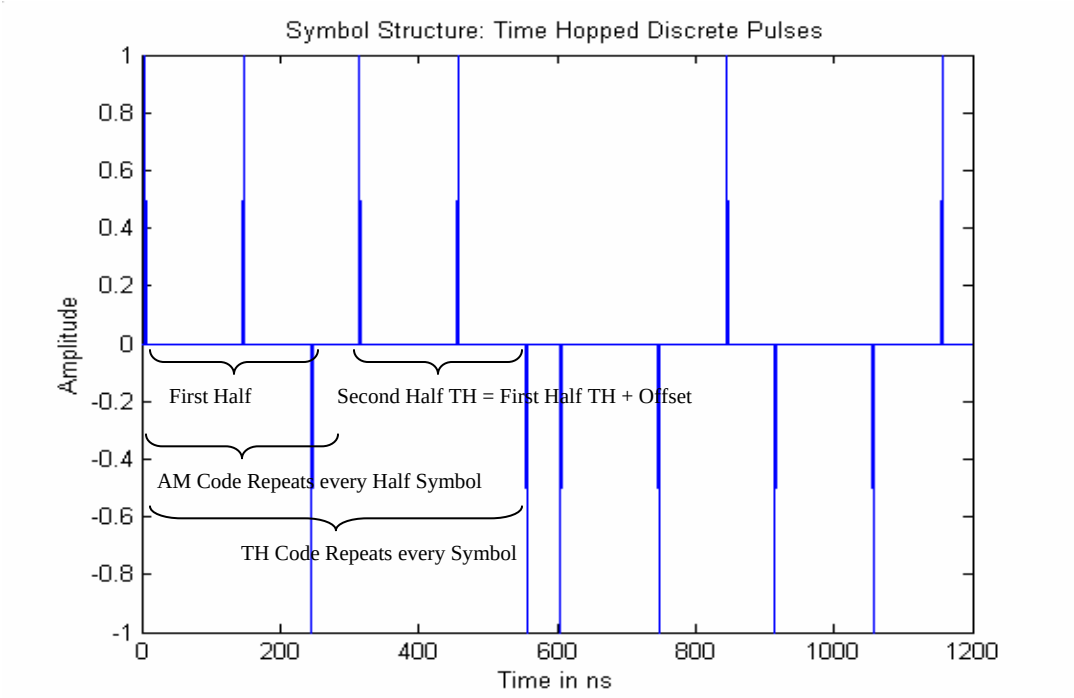

Figure 3.2: Symbol Structure of Time Hopped Discrete Pulse

Now let us consider an interfering user with a code design offset of δ_2. The acquisition process is clearly the same for the interferer, except that the time delay applied to the received signal will be $(N_f/2 + \delta_2)$. In time, if the width of each chip is T_c, the second half of user *i* has to be shifted by $\Delta_i = \delta_i T_c$ to perfectly correlate with the first half. When the interferer's signal is added up with the desired user signal with a random time delay due to path differences, the resulting signal consists of pulses from both users randomly added up. Analyzing this

mathematically, it is found that there are multiple conditions wherein the interfering signal may contribute to the addition.

We already discussed that in the absence of timing error, the peak of autocorrelation occurs at the start or end of each symbol. Since the interfering pulses may add up to the desired user constructively or destructively, the autocorrelation may have maxima at positions other than the start or end of a symbol. This leads to a timing error when the peak-picking of autocorrelation is done. If the number of users in the system is N_u', each chip of the desired user may contain pulses from one or more of the $N_u \equiv (N_u' - 1)$ interferers.

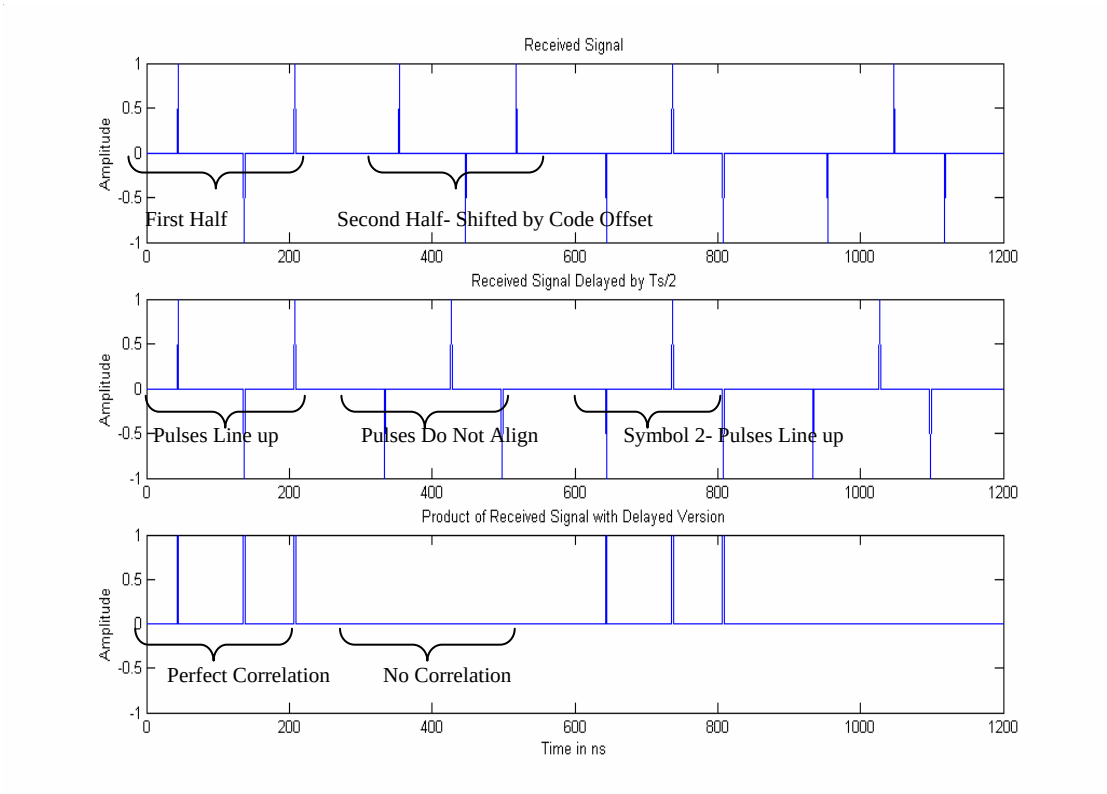

Figure 3.3: Delay and multiply process of received signal

Thus, the time varying autocorrelation function obtained at the time of acquisition may have multiple peaks at various points across [0, N_f*N_c] leading to a different distribution of timing errors. The statistics of this timing error depends on the TH pattern adopted as will be

demonstrated later. It also depends on the signal-to-noise ratio, the number of symbols used for acquisition (M) and also the number of interferers present in the system.

The distribution of mean square error plays an important role in the bit error probabilities of the scheme in multipath and multi-access scenarios. Higher timing errors degrade the BER performance of the code significantly. To illustrate this, we have obtained an expression for the BER of the system conditioned on the timing error, and later averaged this expression using simulation results for the timing error.

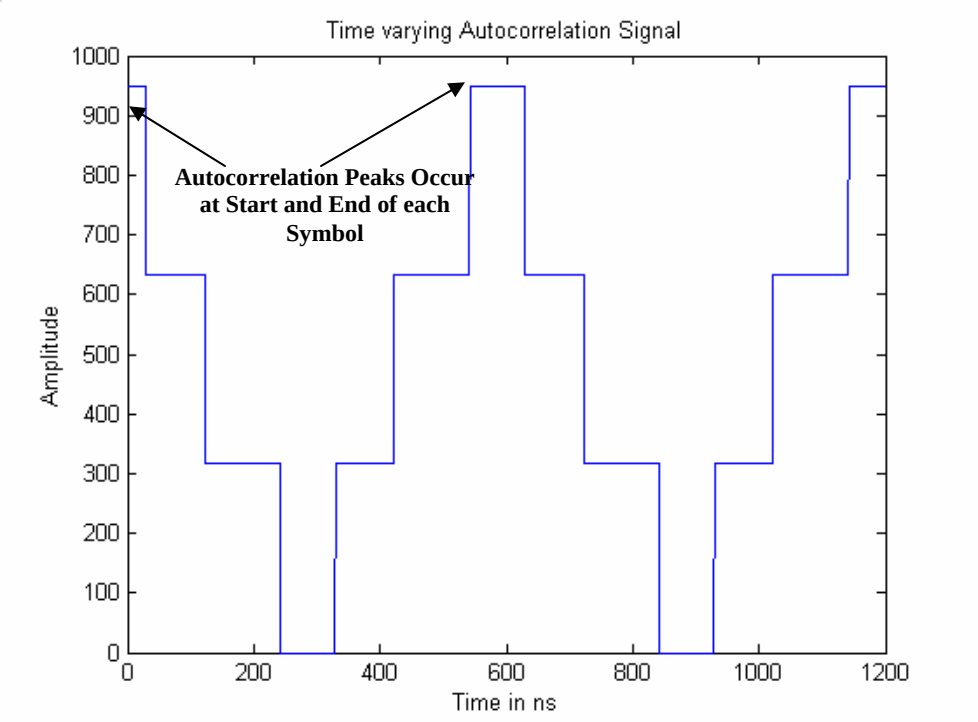

Figure 3.4: Time varying Autocorrelation with Half Symbol Delay

3.3 Advantages and Challenges of the ABS Scheme

One of the important advantages of ABS scheme is that the symbol sequence need not be specified in order to obtain a desired correlation at the receiving end. Compared to earlier schemes, the dependence of timing acquisition on the data symbol sequence has been eliminated. It has also been demonstrated [41] that the ABS Algorithm has the advantage of faster acquisition

speeds as well as lower bit error rates for the same SNR as compared to the existing blind acquisition schemes.

One important challenge of the ABS coding scheme is its performance in the presence of multi-user interference (MUI). Every user needs to be assigned a different value of code design offset (**$\Delta = \delta T_c$**, with δ as an integer**)**. This offset provides users with a separation during the timing acquisition process. As demonstrated earlier, in acquiring the timing using ABS scheme, two half-symbol long windows of the received signal are correlated. The correlation will result in a maximum if the windows contain pulses from the same symbol, and the position of this maximum will occur at the start or end of each symbol. Since each user has a different value for **Δ,** it has to be kept as small as possible to accommodate the maximum number of users. In addition, we need to make sure that the offset timing **Δ** is large enough to ensure that pulses in the two autocorrelation windows are separated, if they belong to different symbols. It has already been proven [41] that under perfect acquisition conditions, the pulses in two windows (with pulses from different users) don't align with each other if separated by 2Δ. Established results also include the fact that the autocorrelation output is very small when **$2\Delta \geq 2$ns, or $\Delta \geq 1$ns.** It is worthwhile to note that with $\Delta_i = \delta i Tc$, the effect of $\Delta_1 - \Delta_2$ on the timing error distribution is minimal.

With the code offsets for different users separated by 0.5 ns and N_c=100, in principle, up to 99 users can be accommodated in the system. This Figure can be improved by increasing the TH spreading gain of the system (N_c), but at the cost of reducing the effective bit-rate. The presence of more users adds to the pulses of the desired user signal as interference. This has the effect of increasing the timing errors after acquisition. The effect of more users on the timing error statistics is strong as will be seen in the forthcoming chapters. Practically, the timing errors limit the simultaneous users to well below 99, as we will quantify.

Most of the focus of existing research on UWB blind timing acquisition has been to reduce the complexity of the code design while improving multiple access capabilities. The

following section introduces a set of four patterns which can be explored for the design of the user TH codes. This is followed by a detailed analysis of the timing error statistics for various TH patterns, signal-to-noise ratios, the number of interferers and number of symbols used for timing acquisition.

3.4 Design of the TH Code

The multiple access capabilities of the system are clearly based on the design of the unique TH code which each user is assigned. In a multi-user scenario, the uniqueness of the TH code is enhanced by an offset (δ_i, for user i) assigned to each users in the second half of its symbols. We have explored the ways of varying the TH code pattern across users by improving the randomness of the frames of each user. Our goal is to achieve a lower timing error compared to cases where all users have similar code patterns. The implementation of amplitude modulation along with different random TH codes improves timing accuracy further. We consider hopping patterns of four kinds as follows:

Uniform Time Hopping, Same Pattern (USTH): Here, the TH code consists of a uniform displacement of pulses in a frame, basically a shift of same number of chips in every frame. Also, each user has as the same pattern as others. The only difference between user codes is the design offset (δ) which is unique for a particular user.

Random Time Hopping, Same Pattern (RSTH): Here, the TH pattern is a pseudo- random sequence of time hops, only all users have the same code pattern. The only difference between user codes is the design offset, which is unique to each user.

Random Time Hopping, Different Pattern (RDTH): Here, a different pseudo-random sequence of time hops is assigned to each user. The unique code design offset in the second half of its symbols enables each user to de-correlate the signal transmitted with correspondence to their code design.

Random Time Hopping, Different Pattern and Amplitude modulation in the frames (RDAM): Here, random and different sequence of TH pattern is assigned to each user. In addition, the pulses are amplitude modulated by a binary code, ±A. Note that the AM pattern in each symbol must be uniform and should repeat every half symbol. Thus, a random amplitude modulation sequence of half-symbol period is assigned to each user. This provides two-tier randomness, one due to the TH, and the other due to the AM code.

3.5 Receiver Processing

To understand the effect of timing error, let us consider how the received signal is processed by the receiver. The essence of timing acquisition lies in determining the start of the symbol to within a frame-time. Channel estimation using maximum likelihood criterion or similar criteria can then be done by correlating a sliding template of the transmitted symbol with the received signal over a frame period to estimate all the delays and the echoes. Thus, if the receiver incurs a timing error of more than one frame time, degradation in bit-error rate can be experienced since a significant fraction of energy will not be captured by correlating the signal template with the received signal.

The scheme is differential in the sense that successive half-symbols are used as dirty templates for each other and used as correlation windows. Starting at a random position in the received signal, the signal is correlated with a delayed version shifted by a half-symbol period. The correlation interval is half-symbol, $T_s/2$. This process is continued for one symbol period after start of acquisition, and the start time corresponding to the maximum of the correlations is selected as the start-of-transmission. If multiple symbols are used for acquisition (say, M symbols), the acquisition interval is M symbol periods. After the correlation stage, the autocorrelations over M successive symbols are added, symbol-by-symbol. This averages out the

false-maxima in the time- varying autocorrelations, and yields a true-maximum, meaning usually, a lower timing error.

The time position of the peak autocorrelation in timing acquisition phase, relative to the start time, is the timing error. The receiver signal is delay-adjusted according to this timing estimate, and data demodulation is then done using differential detection at the symbol level. The received signal is delayed by one symbol time and the delayed and original signals are correlated one symbol at a time. The polarity of each symbol correlation is used to decide if the transmitted bit was a logical ‘0’ or a logical ‘1’.

3.6 Effect of the Multi-path Environment:

In a dense multipath indoor wireless channel, the initial amplitude profile of the received signal can be obtained using a discrete impulse response model [43, 44]. In simple terms, this model represents multipath components as decayed versions of the pulse delayed by the minimum resolvability time. We know that this decay profile repeats in every frame of the symbol, in a similar fashion. Each frame of the received signal thus contains a set of multipath components, decayed in amplitude and delayed in time in a very similar fashion as other frames. Since this multipath power decay pattern repeats itself in every frame, use of differential detection can be very productive. When we correlate two half symbols or two symbols of the received signal at a time, the multipath components in the frames in both correlation windows reinforce each other, a process we call *self-Raking*. It can be seen that amplitude distributions of multipath rays repeat from symbol to symbol, since the multipath channel affects the pulse in each frame in the same way. Thus, when differential detection is used, multipath components in adjacent symbols reinforce each other, thus capturing most of the multipath energy. This simplifies the receiver structure and thus a simple differential detector can be used instead of a complicated Rake receiver with multiple fingers. The ABS scheme timing acquisition performs in a very similar

fashion, irrespective of the channel model used [41]. Under these conditions, we conveniently neglect the effect of multipath effects in our simulations, and assume the multipath components can be assumed to be taken care of by the Gaussian Interference plus Thermal Noise model.

Since we use a differential technique both in acquisition phase (half-symbol long correlation windows) and data symbol-detection phase (symbol-long correlation windows), we can conveniently neglect the effect of multipath interference in all the timing error simulations as well as $_{BER}$ calculations. It was also shown in [41] that the ABS scheme performs almost similarly with any kind of channel model (CM 1-3) being used. All simulations were done assuming a single path for each user and received pulses just noise-corrupted versions of the transmitted pulses.

3.7 Simulation of Timing Error Initial results

The absolute value of timing error, which ranges from 0 to Ts/2, can be a significant source of degradation in BER performance and determining the probability density functions of the timing error and their statistics is critical to assessing detection performance. The following steps were performed in obtaining the timing error distributions:

i. The following sub-steps are performed to generate the signal vector. A set of TH codes is generated for a fixed number of users in the system using the ABS code design. The TH code patterns described in the previous chapter are chosen one at a time. The value of Δ for the desired user signal was assigned to be 1*ns*, even though any other value is acceptable as well. A sequence of i.i.d. binary symbols (± 1) is generated. The sampling interval used is $\Delta T = T_c = 1ns$. $s(k) = s_k = s(k\Delta T)$ where $s(t)$ is the received input signal without the noise. We use discrete pulse with a peak power P_{max} ($=\sqrt{N_c.SNR.P_n}$), where P_n is the noise variance. For analytical simplicity, we assume unit noise variance.

ii. The variance of the interfering users (which is approximated as a Gaussian random variable as will be shown), is N_u*P_{max}/N_c, where N_u is the effective number of users. Once the symbol sequence for the desired user is generated, a Gaussian thermal noise vector of variance $(1+N_u*SNR)$. The noise and interference vector generated is added to the desired user signal vector at chip intervals to obtain the sequence used for timing acquisition. The SNR is defined as the average energy in each chip divided by the noise variance.

iii. According to the proposed algorithm, the autocorrelation vector is obtained through the product of the final sequence obtained from Step 2 and a delayed version of itself. According to the value of M for the trial, the autocorrelation sequence is averaged over M symbols.

iv. As the number of interferers increase, the position of the peak autocorrelation shifts from the start of the symbols. Thus resulting in a timing error. We have defined the absolute timing error to be the difference between the position of autocorrelation and the start of the nearest symbol. Only absolute values of the timing error are considered since the symmetry of plots yields similar results for positive and negative timing errors, as they should.

v. The moments of the timing error are obtained for different TH code patterns and varying number of interferers (N_u). Comparisons are made between different N_u for a particular TH code pattern as well as different code patterns for fixed N_u.

` The autocorrelation obtained by sliding half-symbol long windows may not be maximum at the start of the symbol due to presence of interfering pulses. The timing error or the shift of the maximum autocorrelation from the starting position of the symbol tends to increase with the presence of more users and Gaussian thermal noise. To find the best of the TH codes to use, we

calculate the standard deviation of the timing error with varying number of users in the system. Figure 3.5 shows the comparisons.

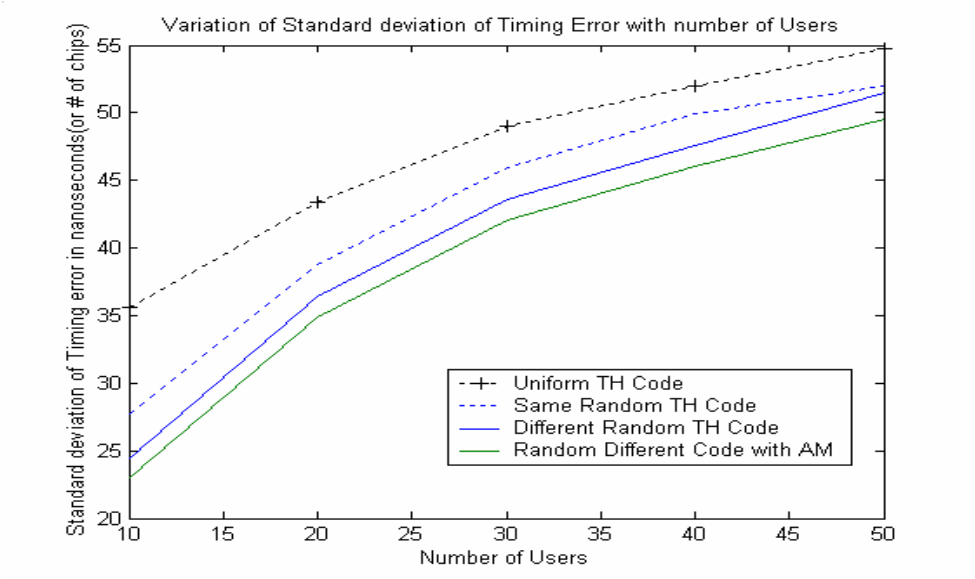

Figure 3.5: Comparisons among TH Codes: Standard deviation vs number of users

We can clearly observe from Figure 3.5, that the Random Different TH Code with Amplitude modulation is the best among the four code patterns considering the standard deviation (in number of chips) of timing error. Moving forward, we use the most efficient TH code pattern, the ***Random Different TH Code with Amplitude Modulation (RDAM)***. In the forthcoming chapter, we illustrate the effect of number of interferers (N_u), SNR and number of symbols used for the acquisition phase (M) on the distribution of the timing error. Following that, we use these distribution results to derive the $_{BER}$ performance of the detection phase in multi-user, multipath scenarios.

3.8 Interference Model

Since the user's and interferers' pulses in any frame have a bipolar amplitude (+A or –A) in any chosen frame, the interfering power may be positive, negative or zero (no interfering pulses in the frame). If there are N_u interfering users, the amplitude of the pulse in the chip can be

modeled as a uniform random variable with discrete values between $-N_u.A$ to $+N_u.A$ with zero mean. By central limit theorem, as the number of users in the system increases, the total amplitude in a chosen chip tends to become Gaussian with a mean of zero.

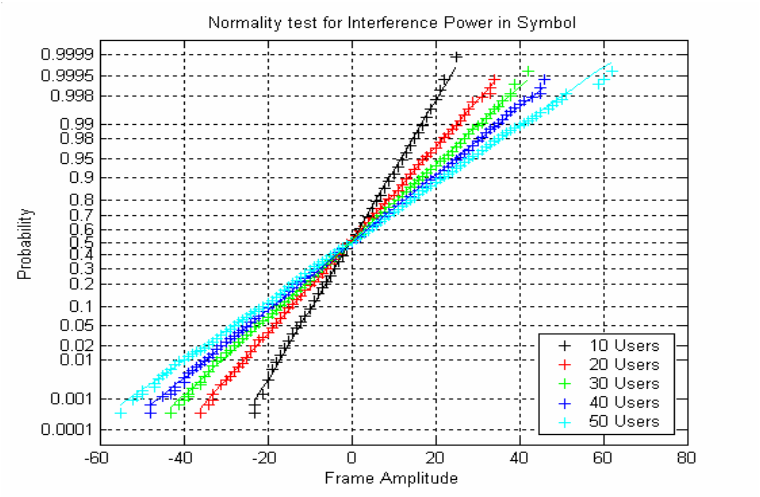

Figure 3.6: Normality tests for Interference Sum terms

This has been verified through simulations, as illustrated in the normality plots in Figure 3.6 and 3.7. As one can notice from the distribution of frame energy, the presence of interference

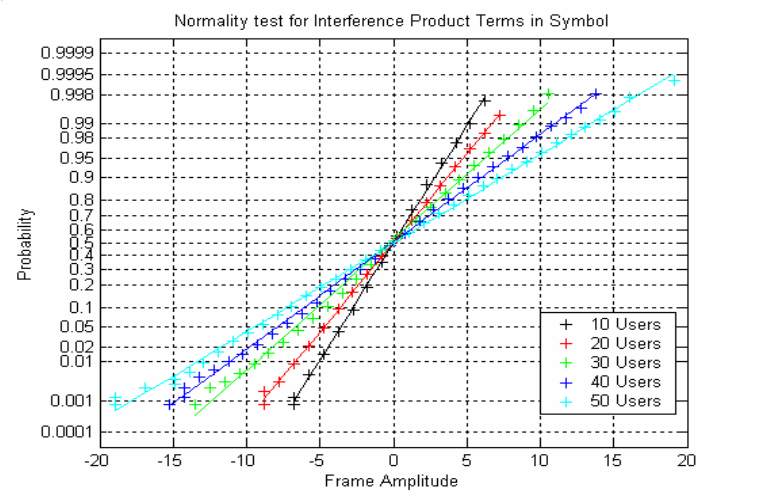

Figure 3.7: Normality test for Interference Product terms

tends to be sufficiently Gaussian even with 10 users and becomes significant with increase in number of users. In the presence of multipath energy in the received signal, this basically consists of weighted delayed pulses of the desired user added back to the same user's transmitted signal.

In this scenario, we can easily notice that the Gaussian assumption of interference per chip is strengthened by the presence of additional energy from multipath rays. Thus moving forward in this thesis, all interference and multipath energy is modeled as single Gaussian interference term. Now the product terms obtained in process of differential detection due to the cross correlation of user and interfering pulses, also tends to be Gaussian in any given chip, as seen in Figure 3.7. Note that both the sum and product terms containing the interfering pulses tend to be Gaussian with zero mean, the variance increasing as the number of users in the system increases.

3.9 Assumptions on Transmit Pulse

The transmit pulse used in all our simulations is a discrete pulse with finite amplitude. We can safely assume a discrete pulse shape for the simulations because considering a transmit filter with a Gaussian filter response and a corresponding matched filter at the receiver, we obtain a second derivative Gaussian pulse at the output of the matched filter. The effective pulse width of this second derivative Gaussian pulse was simulated to be 1.17 ns, which is close to the chip time of 1ns assumed. Detailed derivations to justify the use of a discrete transmit pulse can be found in Appendix A.2. The result and assumptions can be generalized for any transmit pulse shape as long the effective pulse width assumed is close to 1 ns.

Chapter 4

Timing Error Analysis and Results

4.1 Introduction

As discussed in the previous chapter, different TH code patterns were tested via simulations. It has been shown that the cross correlation between two user signals will be minimum when their code design offsets are separated at least by half a chip time [41]. This gives us a flexibility to accommodate N_c*-1* users in the system, if we choose N_c chips per frame. However, the addition of users to the system increases the probability of higher timing error. We will illustrate in this chapter, that the number of effective interferers is the limiting factor on the timing error performance of the ABS algorithm, as compared to the SNR. As an improvement, we incorporate multiple symbols (M) for timing acquisition, which involves averaging the autocorrelation calculated for timing. When averaged over multiple symbols, it will be shown that the absolute timing error reduces. In this chapter, we obtain the cumulative distributions of absolute timing error as a function of N_u, SNR and M.

4.2 Simulation Results

The simulations have been conducted for values of *M=2, 4, 8 and 16*. Five different *SNR* conditions (*5, 10, 15, 20 and 25 dB*) and up to five values of N_u (5, 10, 15, 20 and 25) were considered. In order to achieve realistic transmission, we have made the following system assumptions.

- For simulation convenience, the transmit pulse is the discrete impulse peaking at multiples of the chip-time.

- The frame length is $T_f = 100\ ns$, and each frame has a pulse which is time-hopped among $N_c = 100$ chips, each chip of width $T_c = 1ns$.

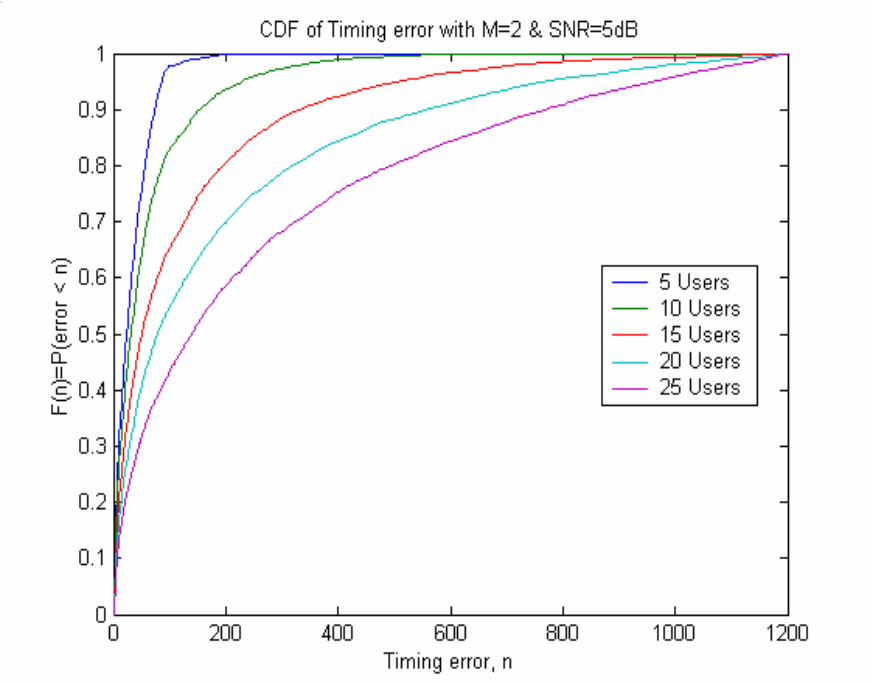

Figure 4.1: Timing Error CDF with M=2 Symbols, SNR=5dB

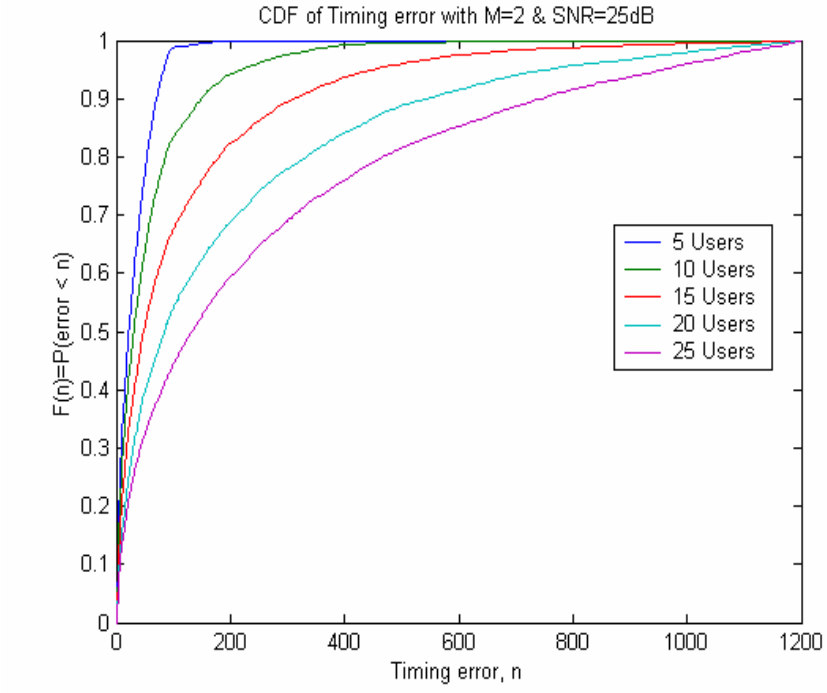

Figure 4.2: Timing Error CDF with M=2 Symbols, SNR=25dB

- The code design offset chosen for the first user is $\Delta = 1$ *ns*. Using the procedure outlined in section 3.7, we have acquired the statistics of absolute timing error under the various conditions.

Figures 4.1 to 4.11 show the simulations results for cumulative distribution function for the timing error, n. Figures 4.1 & 4.2 depict the cumulative distribution functions of Absolute timing error with *M=2* symbols, for SNR=5 dB and 25 dB respectively. We can see that, for a fixed *SNR* and value of *M*, as the number of users in the system increases, the probability of higher timing error increases significantly. With five users in the system, timing errors can be limited to close to a frame. This value of timing error is achieved due to the time hopping in the first frame. If the timing acquisition starts after the position of the pulse in the first frame, the minimum timing error achievable is one frame. The Figures 4.1 and 4.2 depict the effect of effective interferers on the timing error performance of the system, illustrating, that even at a high SNR, the number of effective users is the limiting factor on the timing performance. This result is further supported even with increase in the value of M used for the acquisitions, as will be described.

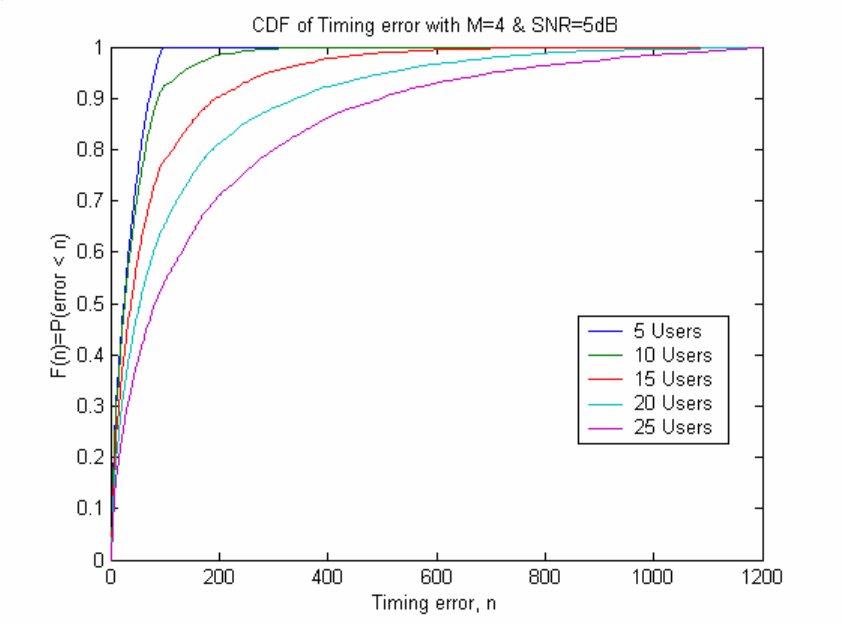

Figure 4.3: Timing Error CDF with M=4 Symbols, SNR=5dB

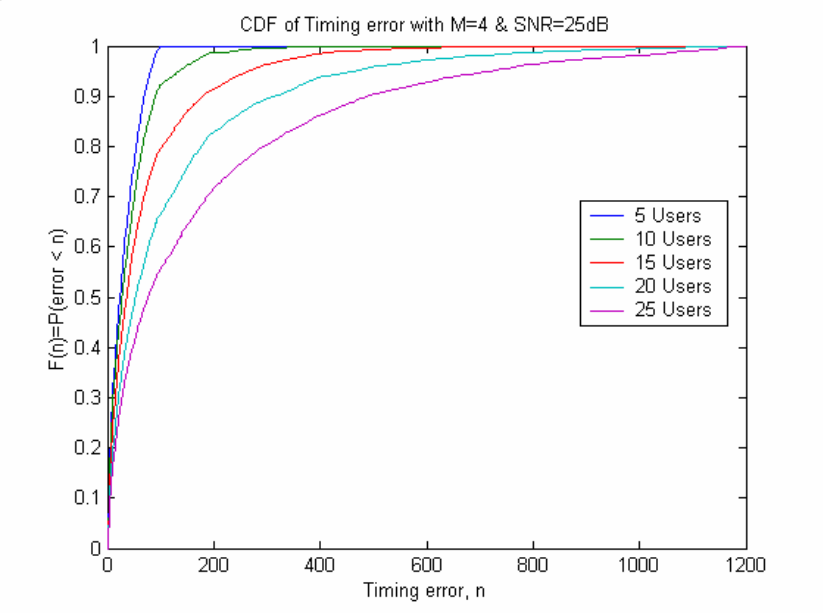

Figure 4.4: Timing Error CDF with M=4 Symbols, SNR=25dB

As can be seen from Figure 4.3, when the number of symbols (M=4) over which autocorrelations are averaged increases, the probability of higher timing errors reduces as compared. Figure *4.3* depicts the timing error CDFs with M=4 and SNR= 5 dB. When the number of users N_u is limited to about 5, the system performance can be improved significantly since most timing errors are of the magnitude of a single frame (100ns). As the SNR is increased to 25 dB, some improvements in timing error performance can be noticed (Figure 4.4). The effect of (or *M*) can be further illustrated in Figures 4.5 and 4.6 which show the CDF of timing errors for M=8 and M=16, respectively, with SNR= 25dB. As can be noticed, for a fixed SNR, significant improvements in timing error performance can be achieved by increasing the number of symbols used for acquisition from M=2 to M=16. Even with up to 25 users in the system at high SNR, timing errors can be limited to four frames, with M=16 symbols used for timing acquisition.

Figures 4.7 and 4.8 demonstrate the effect of SNR on timing error for fixed values of *M* and N_u. It is evident from these results that, the effect of SNR on the timing error distributions is significantly lesser than the effect of interfering users, even with increasing values of *M*. Comparing the results from Figures 4.7 – 4.9, we can say that for low number of users in the

system, even when the SNR is too minimal, there is a small probability of getting huge timing errors. In this case, all values of M give the same result and timing errors are limited to one frame time. With N_u=5 users in the system, the timing error distributions for lower SNRs or values of M are significantly small compared to N_u=10 users or more.

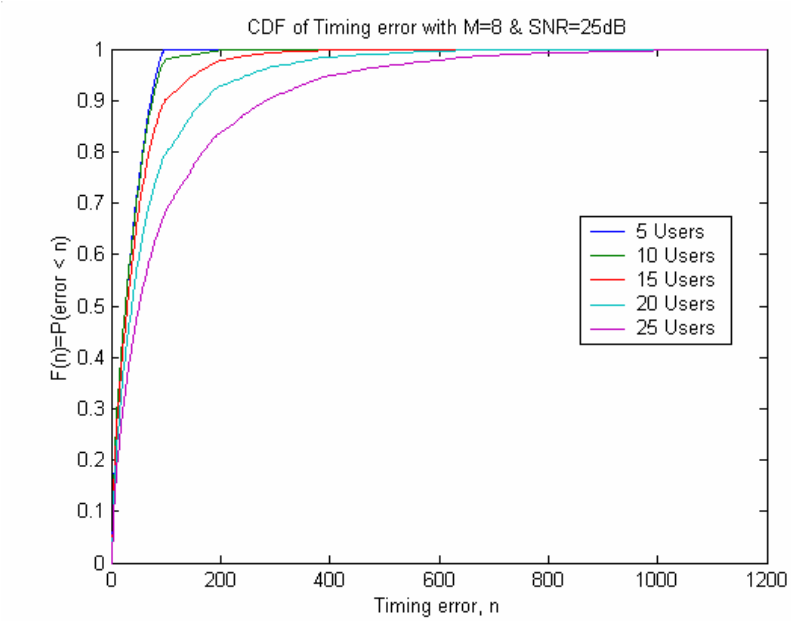

Figure 4.5: Timing Error CDF with M=8 Symbols, SNR=25dB

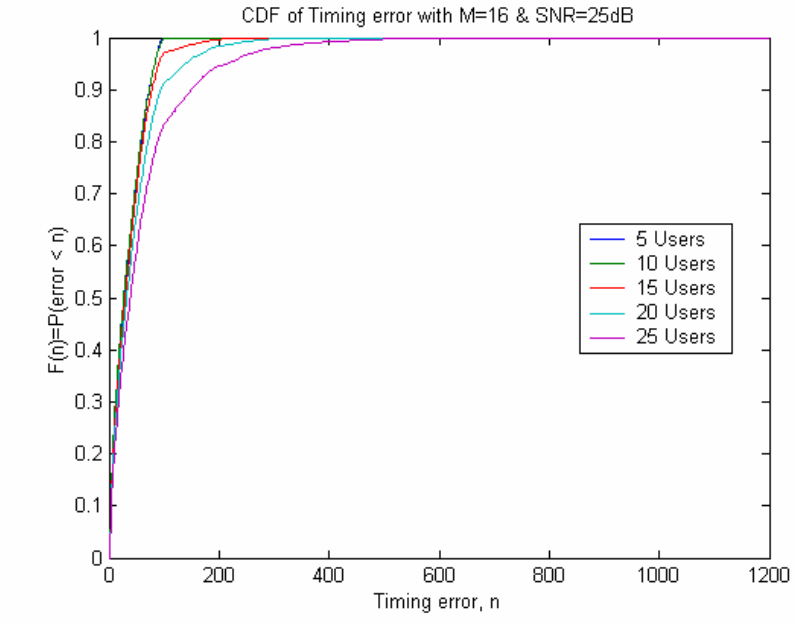

Figure 4.6: Timing Error CDF with M=16 Symbols, SNR=25dB

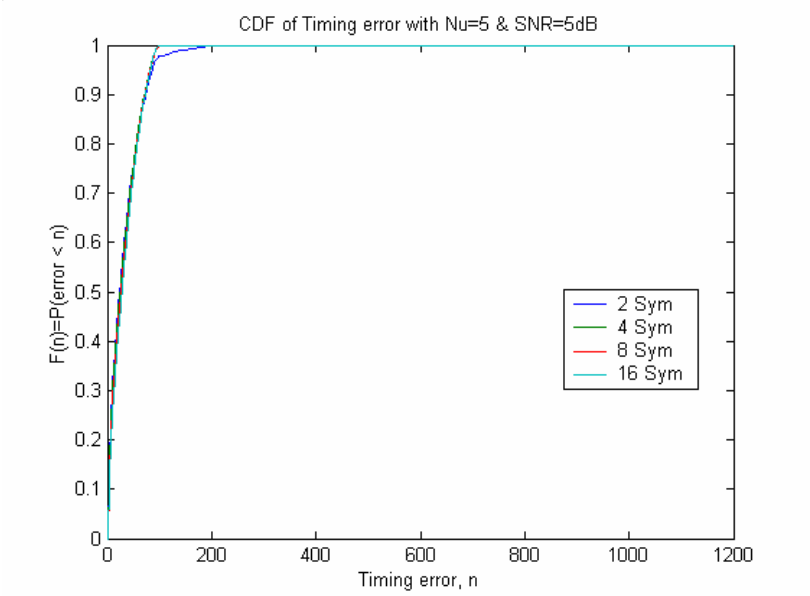

Figure 4.7: Timing Error CDF with SNR=5dB, N_u=5 Users

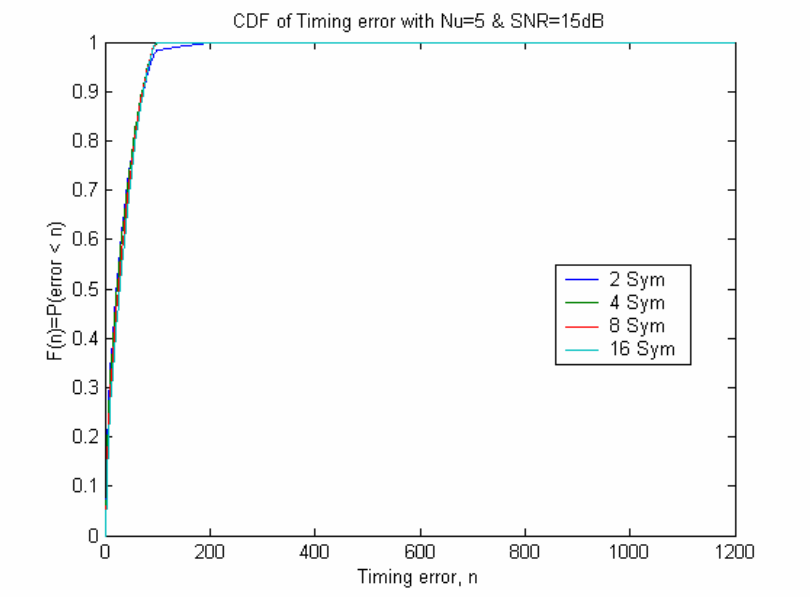

Figure 4.8: Timing Error CDF with SNR=15dB, N_u=5 Users

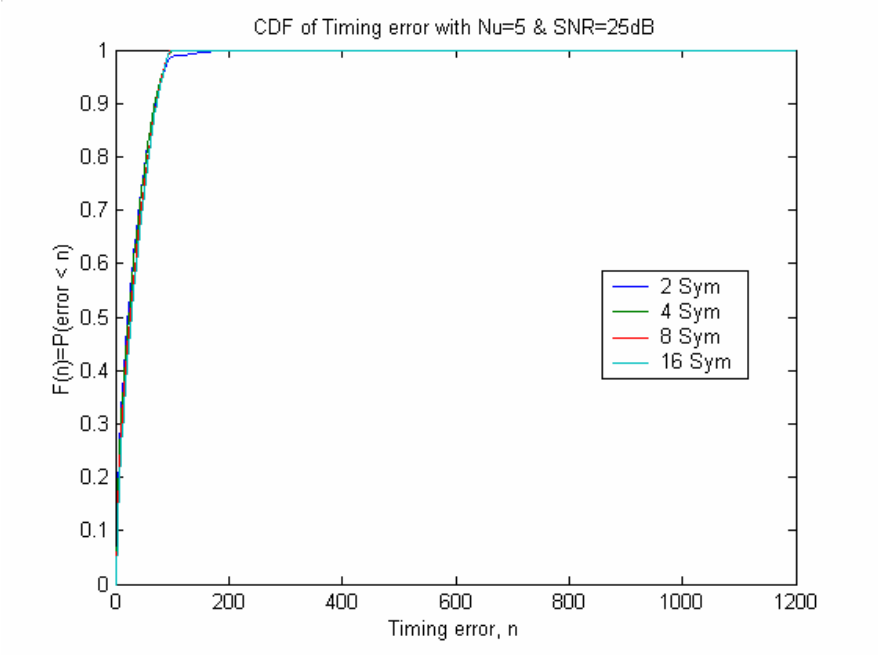

Figure 4.9: Timing Error CDF with SNR=25dB, N_u=5 Users

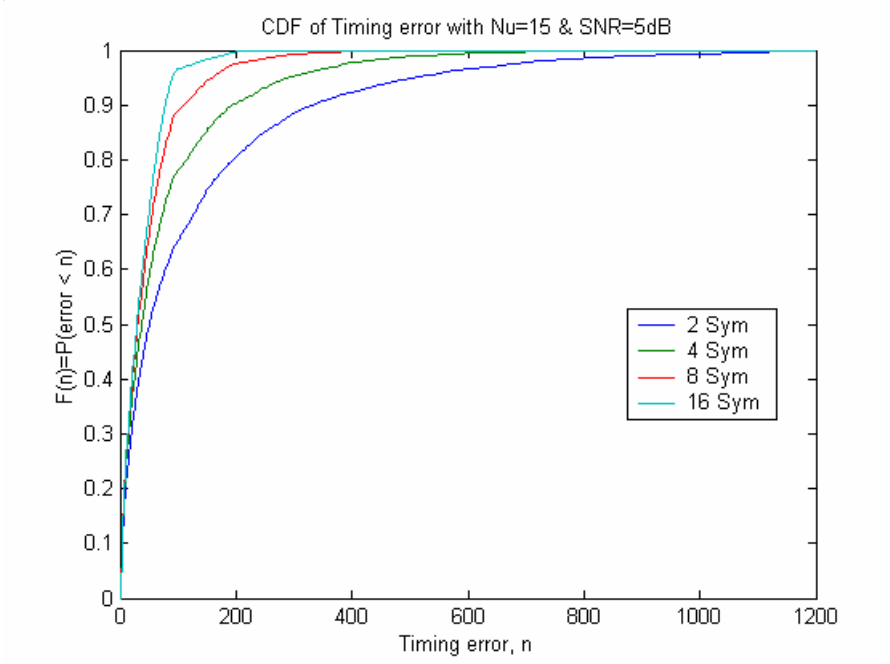

Figure 4.10: Timing Error CDF with SNR=5dB, N_u=15 Users

The effects of the interferers can be further stressed through results obtained for higher values of N_u as shown in Figures 4.10-4.14. Note from Figure 4.10, that even with SNR of 5dB, and N_u=15 users, the higher values of timing errors can be significantly reduced by increasing M

up to 16. Various results, shown for different values of N_u, M and SNR, indicate that even at very high SNR values the timing error performance gets limited by the number of users N_u. Figures 4.11-4.14 show that for M=8, 16, the values of error can be maintained low, under low SNR as well as high MUI conditions.

The effects of timing error on the $_{BER}$ performance of the receiver are prominent. In the next chapter, we consider the detection performance of the receiver, measured in terms of BER vs SNR. The BER conditioned on timing error, n is derived and we average the conditional BER over n, using the results obtained in this chapter.

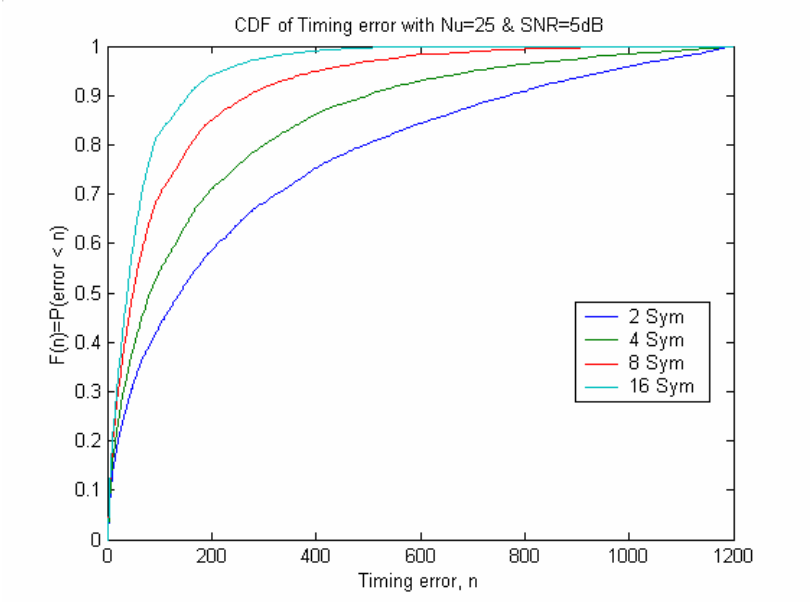

Figure 4.11: Timing Error CDF with SNR=5dB, N_u=25 Users

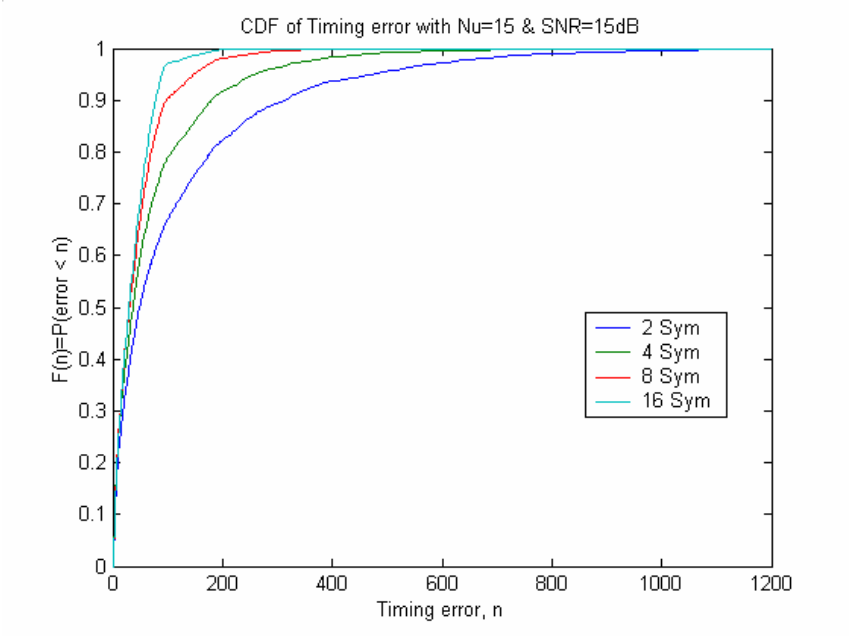

Figure 4.12: Timing Error CDF with SNR=15dB, N_u=15 Users

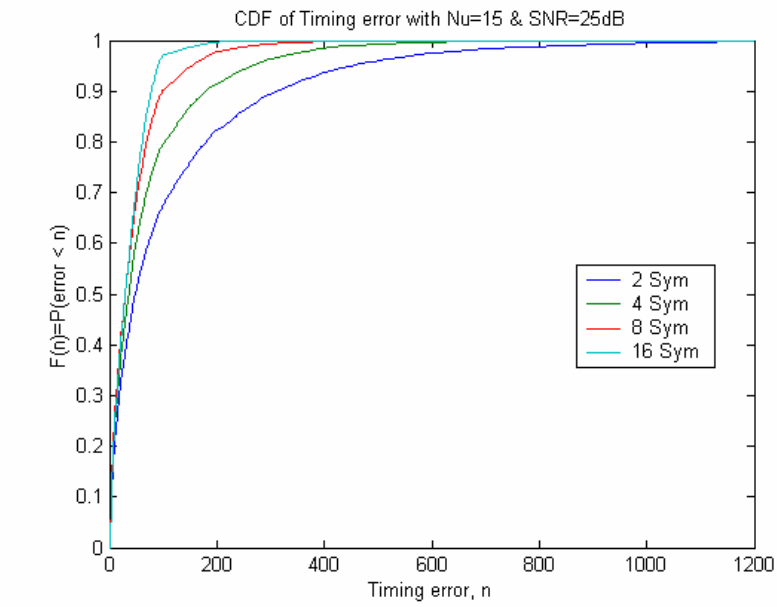

Figure 4.13: Timing Error CDF with SNR=25dB, N_u=15 Users

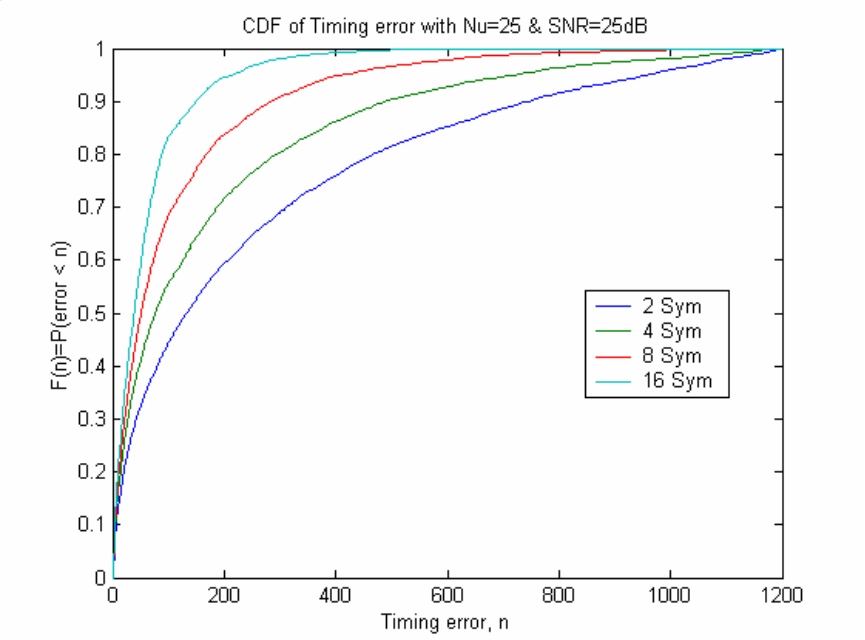

Figure 4.14: Timing Error CDF with SNR=25dB, N_u=25 Users

Chapter 5

BER Performance of Symbol Detection

5.1 Synopsis

Differential detection has been proposed for UWB signal detection [42] as well as timing acquisition. This helps the system Rake most of the multipath energy while relaxing the stringent implementation requirements. This chapter describes in detail the receiver architecture used to regain the data sequence transmitted using differential detection, and presents an analysis of BER performance. For comparison purposes, the ideal Rake receiver is analyzed and average BER performance for ideal Rake reception is plotted. In addition the relationship between data rate and N_u is illustrated for both differential detection as well as Rake reception.

The received signal is corrupted by multi-path interference [44, 45] and thermal noise [43]. In the UWB receiver, the signal acquisition using the 'dirty template concept' can be performed using analog correlators. The timing acquisition phase acquires an accurate estimate of the start of a symbol, and with the predicted symbol start, the receiver begins estimating the data sequence. The importance of timing accuracy is to be noted here, since any timing error greater than one frame time may cause a degradation of the bit error probability.

5.2 System Model & Receiver Architectures

The differential detector we consider is a DPSK receiver (Figure 5.1) and requires differential encoding of the data sequence at the transmitting end. At the receiver, the correlation is calculated between two adjacent symbols using a delay of one symbol time. The resulting correlation sum is compared to a decision threshold to decide if the transmitted bit was a logical '1' or a logical '0'. Under our assumed binary modulation, the decision threshold is zero.

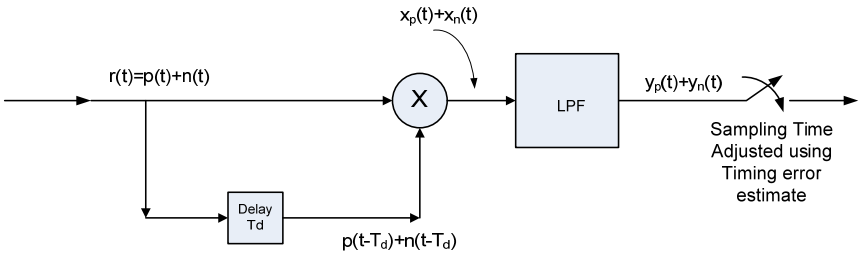

Figure 5.1: Standard DPSK/ Differential Detector Receiver Architecture

It has been established that the differential detector shown here it helps capture most of the multipath energy present in the frames, as all the multipath energy in a frame is spread only in the frame period. This helps the differential detector receiver *self-Rake* the received signal, thus avoiding the need for a channel-estimating Rake receiver. The self-Raking process has already been described earlier. The use of a DPSK differential detector also eliminates the need to include detailed multipath considerations in the mathematical analyses. That is, the use of the differential detector makes the BER results independent of the channel profile.

The receiver shown in Figure 5.2 depicts the two-stage Detector, using the differential technique for both timing acquisition and data detection. For simplicity, the details of ABS scheme are not shown, but it is conveniently assumed that the timing estimate obtained from the synchronization stage is used in the detection phase. It is to be observed that the same principle of *self-Raking* applies to the interference energy present in the frames. Thus the differential detector has the drawback of increasing the overall noise floor due to *self-Raking* of the interference energy.

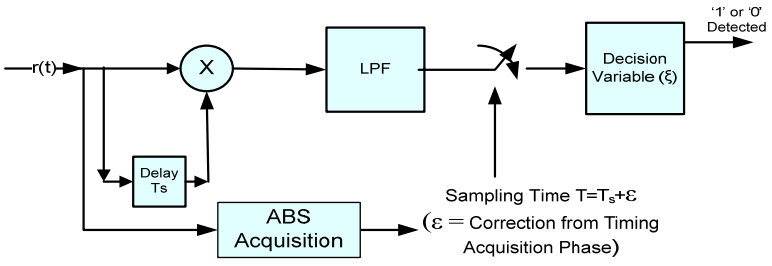

Figure 5.2: DPSK Receiver Architecture with Differential Signal Acquisition Phase

To prevent this from overly affecting the decision making, we propose a small modification at the transmitter, wherein the N_f pulses in alternate data symbols are either delayed or advanced by Δ_i (code design offset assigned uniquely to each user i). For example if the current transmitted symbol has a particular TH code, the next symbol has the same code with additional time delay of Δ. Thus in each symbol there are two uses of Δ: the second half of each symbol is delayed from the first half by Δ for timing synchronization purposes and the overall symbol is given an additional delay of Δ or (-Δ) for avoiding the *self-Raking* of interference energy at the receiver. Since all the frames of each symbol are shifted and Δ is uniquely chosen for each user in the system, this process does not affect the timing acquisition phase. This helps the DPSK receiver to avoid capturing the multipath components of the interferers and thus improves the BER performance via increasing SINR.

A modified receiver structure to accommodate the change suggested at the transmitter is shown in Figure 5.3. It consists of the ABS timing acquisition phase, followed by a data detection stage which has a CRC feedback circuit. In a regular data detection phase, the received signal is correlated with a delayed version of itself, shifted by a symbol period (T_S). In the modified structure #1, since the transmitted symbols have an additional delay of ±Δ, the currently received symbols are given a delay of either +Δ or -Δ and a CRC feedback loop is used to toggle the delay according to the errors obtained. The CRC loop is used to check if the current symbol being detected has been given the correct additional offset (+Δ or -Δ). If the delay is correct, CRC detects lower errors and the delay is toggled.

Another different implementation strategy can be implemented to realize this change in the transmitter. The modified structure #2 of a differential detector is shown in Figure 5.4. This proposed structure consists of delays and correlators. The received signal is split into four arms, with a delay of +Δ, -Δ, $T_s/2$+Δ or $T_s/2$-Δ respectively. The timing of the received signal r(t) is estimated with a finite timing error (*n*) to obtain r'(t). r'(t) is now split across the four arms of

delays, giving rise to four delayed versions, r'(t-Δ), r'(t+Δ), r'(t-T_s-Δ) and r'(t –T_s+Δ). Now the correlators are used to find the two products, ξ_1= (r'(t-Δ) & r'(t-T_s+Δ)) and ξ_2 = ((r'(t+Δ) & r'(t-T_s-Δ)).A decision device is then used to estimate the data symbol that was transmitted depending on the outputs ξ_1 or ξ_2. The modified receiver structures provide all the advantages of the original differential detector with an additional advantage of avoiding interference multipath energy being captured. In all our analyses and simulations, we have assumed this change has been implemented.

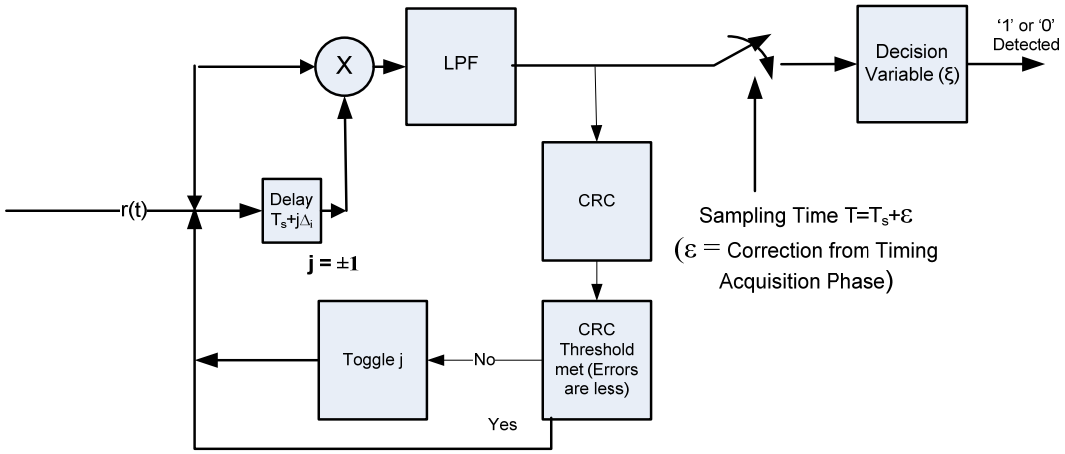

Figure 5.3: Modified DPSK Receiver Architecture#1

The effect of the timing error on the BER performance of the receiver shown above is quantifiable. We have derived BER as a function of the number of users conditioned on the timing error; and averaged the BER over the timing error distribution, using results obtained from the simulations in Chapter 3. As we will see in the results, when this detection scheme is used, the timing error incurred is not a limiting factor on the BER performance. The dominant factor, with or without timing errors, is the dramatic decline in SINR with increasing number of users.

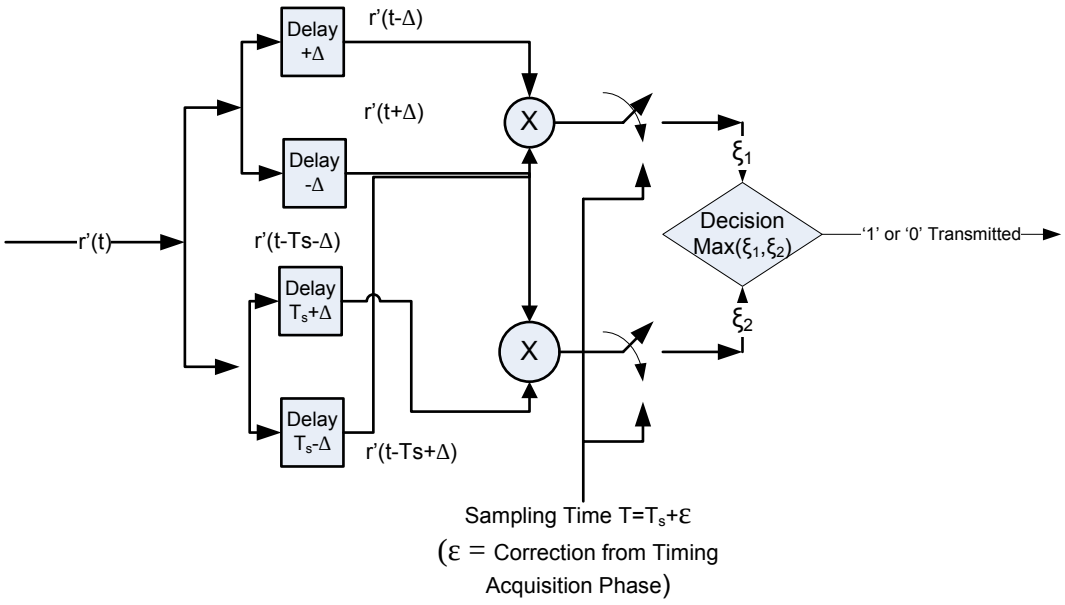

Figure 5.4: Modified DPSK Receiver Architecture#2

5.3 Bit Error Rate: Theoretical Analysis

We have developed a simple analysis to calculate the decision variable and BER for differential detection in the presence of multiple users and a finite timing error for the desired user. Let N_t be the total number of chips in a symbol, N_f be the number of frames per symbol; and N_c be the number of chips per frame. Let s_{ij} and n_{ij} denote the signal and noise components of the i^{th} frame and j^{th} symbol. In differential detection, the decision variable is calculated by correlating two symbol-long windows, starting from the acquired timing position, (assuming that as the start of symbol 1).

5.3.1 BER with No Timing Error

In the absence of timing error, the decision variable is obtained from symbols 1 and 2 alone as,

$$\varepsilon_T = \sum_{i=1}^{N_f} (S_{i1} + N_{i1})(S_{i2} + N_{i2}) \qquad \text{..... (5.1)}$$

where S_{i1} is the i^{th} frame amplitude of symbol 1 and S_{i2} is i^{th} frame amplitude of symbol 2. The noise components are N_{i1} in the i^{th} frame of symbol 1, N_{i2} in the i^{th} frame of symbol 2.

It is to be noted that the noise components N_{i1} and N_{i2} include both the thermal noise in the receiver as well as the multi-user interference. Simplifying this expression,

$$\varepsilon_T = \sum_{i=1}^{Nf} (S_{i1}S_{i2}) + \sum_{i=1}^{Nf} (S_{i2}N_{i1} + S_{i1}N_i + N_{i1}N_{i2}) = \boldsymbol{S} + \boldsymbol{N}$$

where $\boldsymbol{S} = \sum_{i=1}^{Nf} (S_{i1}S_{i2})$ is the signal component and $\boldsymbol{N} = \sum_{i=1}^{Nf} (S_{i2}N_{i1} + S_{i1}N_i + N_{i1}N_{i2})$ is the overall noise plus interference component.

It can be easily shown that $\boldsymbol{N}$ is independent of $\boldsymbol{S}$; $\boldsymbol{N}$ is a zero mean random variable with known variance. Also, under a dense multipath environment with many users, N approaches a Gaussian distribution via the central limit theorem. Now the decision of the receiver about the data symbol transmitted is dependent on the decision variable ε_T as follows:

1. If $\varepsilon_T \geq 0$, no change is transmitted between current and next data symbol (or data='0').
2. If $\varepsilon_T < 0$, a change is transmitted between current and next data symbol (or data = '1')

In the presence of a timing error, the detection is affected, as the timing error determines the amount of desired signal energy captured by the receiver. Moving forward, we will separate the interference terms I_i from the noise N_i in each chip i of a frame. If n chips of timing error has occurred after timing acquisition, the decision variable is then calculated as $\boldsymbol{S} + \boldsymbol{N}$ where,

$\boldsymbol{S}$= signal component = $\sum_{i=1}^{NcNf-n} (S_{i1}.S_{i2})$

and $\boldsymbol{N}$ is the noise component consisting of thermal noise terms(N_{i1},N_{i2},N_{i3}) as well as multi-user interference $I_{i1} = \sum_{j=1}^{Nu} I_{j1}$, where N_u is the number of interferers. I_{i1} contains discrete pulses from all interferers in the i^{th} chip. Both terms of the above equation will contribute to sum and product terms of the Gaussian thermal noise and interfering pulses in each chip. The variance of the sum of the interfering and noise terms can be calculated by considering only the terms contributing to the total Gaussian interference plus noise energy in a chip:

$$\sigma_{ni}^{\,2} = \sum_{i=1}^{NcNf} \mathrm{var}(S_{i1}N_{i2}) + \sum_{i=1}^{NcNf} \mathrm{var}(S_{i2}N_{i1}) + \sum_{i=1}^{NcNf} \mathrm{var}(S_{i1}I_{i2}) + \sum_{i=1}^{NcNf} \mathrm{var}(S_{i2}I_{i1}) + \sum_{i=1}^{NcNf} \mathrm{var}(I_iN_{i2}) + \sum_{i=1}^{NcNf} \mathrm{var}(I_{i2}N_{i1}) + \sum_{i=1}^{NcNf} \mathrm{var}(N_{i1}N_{i2}) + \sum_{i=1}^{NcNf} \mathrm{var}(I_{i1}I_{i2})$$

……. (5.2)

Combining terms and simplifying the expressions because of symmetry from chip to chip,

$$\sigma_{ni}^{\,2} = 2\sum_{i=1}^{NcNf}\mathrm{var}(S_{i1}N_{i2}) + 2\sum_{i=1}^{NcNf}\mathrm{var}(S_{i1}I_{i2}) + 2\sum_{i=1}^{NcNf}\mathrm{var}(I_iN_{i2}) + \sum_{i=1}^{NcNf}\mathrm{var}(N_{i1}N_{i2}) + \sum_{i=1}^{NcNf}\mathrm{var}(I_{i1}I_{i2})$$

…….. (5.3)

Where S_{ik}, N_{ik} and I_{ik} are the signal, thermal noise and interference energies in the i^{th} chip of the k^{th} symbol used for the detection process. Assuming equal powers received from all users*, we can express the total variance of the interference and noise in simple terms. If P_u is the desired user pulse peak power and single-sided noise spectral density per frame is N_0,

$$\sigma_{ni}^{\,2} = 2(N_O)(\frac{P_u}{N_c})N_f + 2(P_u)(\frac{N_uP_u}{N_c})N_f + 2(N_O)(\frac{N_uP_u}{N_c})N_f + +(\frac{N_O^{\,2}}{N_c^{\,2}})N_fN_c + (\frac{N_u^{\,2}P_u^{\,2}}{N_c^{\,2}})N_fN_c$$

…….. (5.4)

Using the variance of the Gauss-like sum of chip interference and thermal noise derived above, the signal-to-interference-plus-noise ratio (SINR) with no timing error can be defined as the ratio of the variance of signal component in each term of Eq.5.3 to the total variance derived above.

In the absence of timing error (n=0), the variance of the signal component in the decision variable is $N_f^{\,2}.\,P_u^{\,2}$. The SINR is then,

$$\mathrm{SINR}_{\mathrm{no\_timing\_error}} = \frac{N_f^{\,2}.\,P_u^{\,2}}{\sigma_{ni}^{\,2}} \qquad \text{..……. ..……..(5.5)}$$

---

*We consider unequal powers later, Section 5.4.

Using (4.5),

$$\mathrm{SINR}_{\mathrm{no\_timing\_error}} = \frac{\mathrm{N_f N_c}}{\left(2\left(N_u + \frac{1}{SNR}\right) + \left(N_u + \frac{1}{SNR}\right)^2\right)} \quad \text{. . ……..(5.6)}$$

Consequently, the BER in the presence of no timing error can be given by,

$$\mathrm{BER_{ideal}} = \mathrm{Q}\left(\sqrt{\mathrm{SINR}_{\mathrm{no\_timing\_error}}}\right)$$

$$= \mathrm{Q}\left(\sqrt{\frac{\mathrm{N_f N_c}}{\left(2\left(N_u + \frac{1}{SNR}\right) + \left(N_u + \frac{1}{SNR}\right)^2\right)}}\right) \quad \text{……...…..(5.7)}$$

5.3.2 BER with Timing Error

As proven in earlier sections, the interference terms (sum and product terms) will yield independent Gaussian terms from chip to chip. They can thus be simply combined with white Gaussian noise.

The decision variable in the presence of a timing error of n chips can be given by,

$$\xi = \sum_{i=1}^{N_c N_f - n} (S_{i1} + I_{i1} + N_{i1})(S_{i2} + I_{i2} + N_{i2}) + \sum_{i=1}^{n} (S_{i2} + I_{i2} + N_{i2})(S_{i3} + I_{i3} + N_{i3})$$

…….. (5.8)

Using the regular detection hypotheses of a differential detector derived earlier, the BER with no timing error can be expressed as in equation 5.9.

In the presence of timing error of *n* chips, BER conditioned on the timing error can be calculated from equation 5.7 as,

$$\mathrm{BER}_{\mathrm{n}} = \frac{1}{2} Q\left[\sqrt{\frac{(N_c N_f - 2n)}{2\left(N_u + \frac{N_c}{snr}\right) + \left(N_u + \frac{N_c}{snr}\right)^2}}\right] + \frac{1}{2} Q\left[\sqrt{\frac{(N_c N_f)}{2\left(N_u + \frac{N_c}{snr}\right) + \left(N_u + \frac{N_c}{snr}\right)^2}}\right]$$

…….. (5.9a)

As seen in the detailed expressions, the term evolving from the product of desired pulses from the second and third symbols of the desired user tends be make the overall noise term deviate from the assumed Gaussian behavior. But since this term can take just two values ($\pm A^2$) with equal probability, we have averaged the overall probability over these two cases. In addition to this, we have also considered the chance of the timing error in frame one of the first symbol (where detection is started), being greater than the TH in that frame. This causes the pulse in that frame to be missed. If the TH in first frame is n chips and N_c is the total number of chips in the frame, the chance of including the first pulse is n/N_c and the probability of missing it is $(N_c-n)/N_c$. The decision variable and thus the SNR will be different in these two cases by the energy of a single pulse and can be easily averaged out using the specified probabilities. This probability also exponentially increases as pulses from more frames are missed due to higher values of timing error.

As illustrated, the timing error causes the BER expressions to be skewed from the perfect acquisition scenario. This probability of bit error for a given timing error n, obtained via the simulations is averaged over the distributions of *n*, which has been described in chapter 3.

5.4 System Assumptions

In previous sections the Gaussian assumption of interference was explained. This assumption was proven valid by considering the sum of pulses in each chip, assuming the user and interfering pulses to be discrete or very narrow with finite amplitude. Hence, the random sum of the interference in each chip is independent from one chip to another, and follows a Gaussian distribution. In light of this assumption, we can consider the Interference in each chip added to the thermal noise in each chip, to be one single Gaussian random variable. We noticed that this Gaussian approximation is strengthened as the number of users N_u increases. Also, in the presence of multipath interference, the multipath components in each chip increase in number (on average), thus making the Gaussian approximation even more valid.

Now consider the case of unequal interference powers. Under our assumptions of equal received power, the total interference power is $N_u P_u$, where P_u is the desired user's receive power. Assuming now that ith user has arbitrary receive power P_{ui}, the total interference power is $\sum_i P_{ui}$. Equating this to $N_u P_u$, we can say that the effective number of users in any environment is

$$N_{u,eff} = \frac{\sum_{i=1, i\neq d}^{Ntot} P_i}{P_u} \qquad \text{……..(5.10)}$$

This reinforces the *BER* analysis even when the interfering users are of unequal receive powers because now only the total interfering power, $\sum_{i=1, i\neq d}^{Nu} P_i$ is important. Thus, the Gaussian approximation holds even when when different users are received at different powers. Henceforth, we will use N_u in place of $N_{u,eff}$.

5.5 Results and Comparisons

Exhaustive BER vs SNR curves were simulated for varying conditions of the system. The primary detection scheme used was the conventional differential detector. The BER expression conditioned on the timing error was analytically derived. Overall BER was plotted by averaging the analytical expression using the timing error PDFs for varying system conditions.

Figure 5.5 depicts the BER curves for no timing error. Here, perfect acquisition is assumed and equations for zero timing error are used to plot BER according to the number of users in the system. We notice that, as the number users reaches 25, BER worsens beyond acceptable limits ($>10^{-2}$), even without timing errors. We thus limited the maximum number of users to 25. More users can be accommodated by varying the spreading gain of the system (N_c or N_f) as discussed earlier, but at the cost of reducing the effective data rate of transmission.

In each of the simulations, the timing error was dependent on the code pattern used. We have used RDAM pattern since it was chosen to be the best among all patterns. But even with the best code pattern used and high SNR conditions, the presence of high effective number of users causes more bit errors in detection. For each increment of interferers by 10, the SNR required to maintain a fixed BER raises by 1 dB, approximately.

Also, the users may have non-uniform receive powers, but the differential receiver ignores this non-uniformity. Since the sum of all interferers is assumed to be Gaussian, the varying power profile of interferers is not significant. In addition, the effect of multi-path components on these BER curves is assumed to be minimal due to the self-Raking at the receiver as discussed earlier.

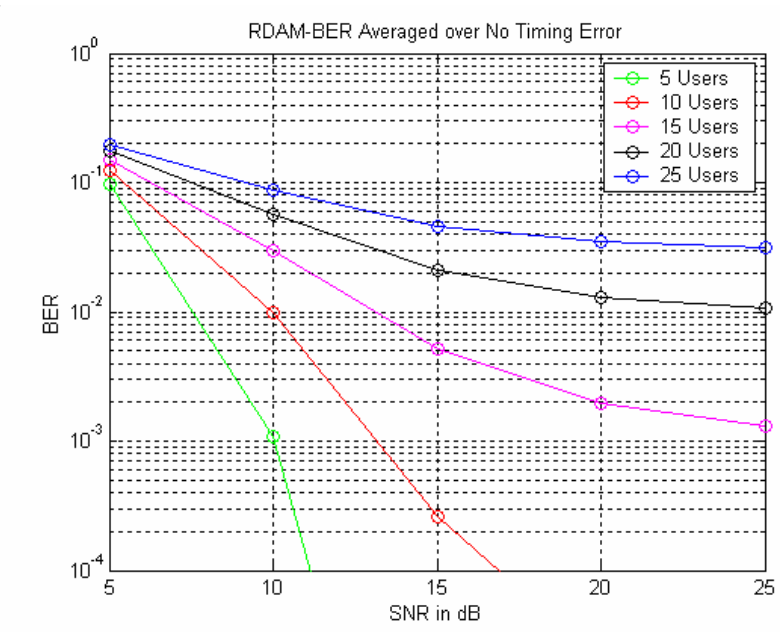

Figure 5.5: BER vs SNR for Increasing N_u, With No Timing Errors

Figures 5.6-5.9 show the BER plots averaged over timing error. As discussed in chapter 4, the timing error distributions are a function of number of users N_u, SNR and M. When M is fixed, the increase in the number of users in the system degrades the BER. Also the BER reduces and reaches a saturated floor for higher values of SNR.

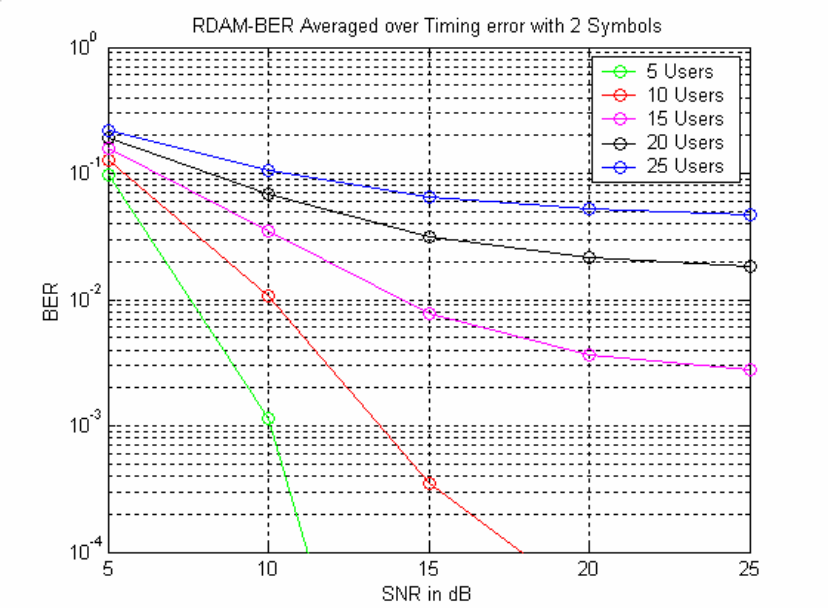

Figure 5.6: BER vs SNR for Increasing N_u, with M=2 Symbols

It is interesting to note, from Figures 5.6 to 5.9, that the limiting factor on BER performance of the detector is the effective number of users N_u. The timing errors incurred after using the ABS scheme for acquisition doesn't cause a significant drop in BER. Rather, it is the interference from other users which degrades the performance of the differential detector. Thus, the BER performance is almost unchanged with the use of M=2, 4, 8 or 16 symbols since the limiting factor is N_u. All the results show that the effect of N_u on the BER performance is similar even if higher values of M are used. Nonetheless, the ABS scheme is definitely an advantage since it performs better and faster than other existing blind TDT schemes, avoiding further degradations to the BER performance.

More results are shown in Figures 5.10 -5.13, which depict the effect of M on the BER performance in the presence of timing errors as compared to the ideal case with no timing error. As Nu increases to 25 and more, the BER is worse than 10^{-2}, even with perfect timing. With timing errors and M = 2, BER performance worsens noticeably, whereas using M = 16 provides BER performance close to the perfect timing case. Compared to the perfect timing case, the

M=16 case performs much better than M=2 case. For a fixed N_u, the influence of M on the BER values becomes discernible only at higher interference levels.

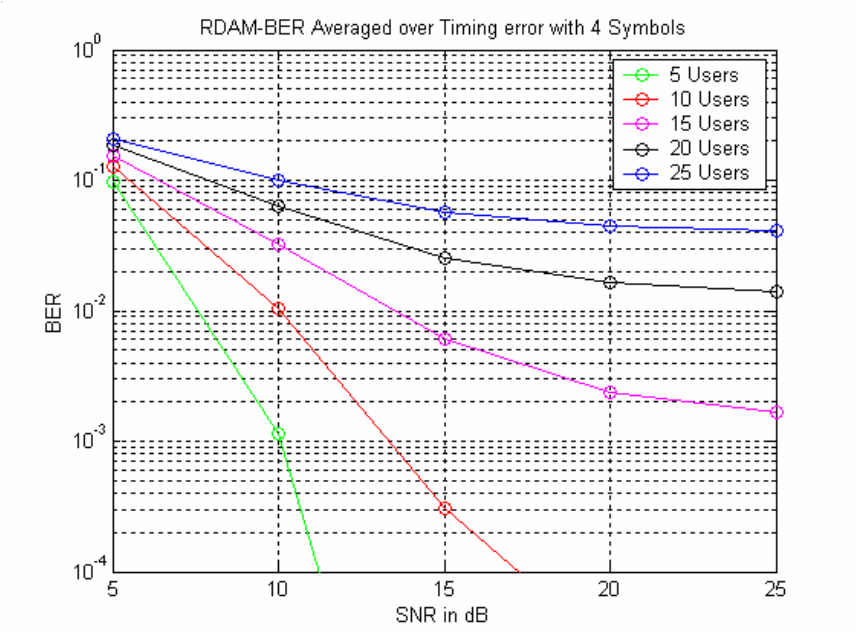

Figure 5.7: BER vs SNR for Increasing N_u, with M=4 Symbols

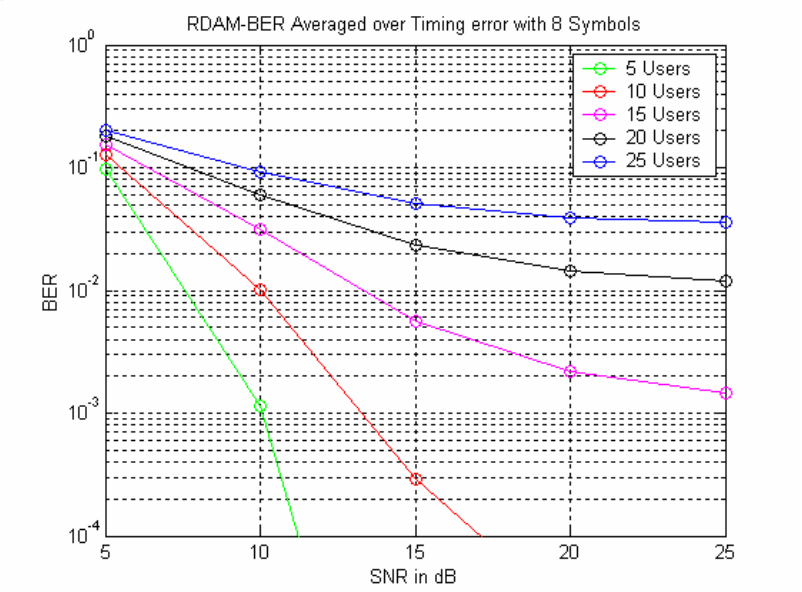

Figure 5.8: BER vs SNR for Increasing N_u, with M=8 Symbols

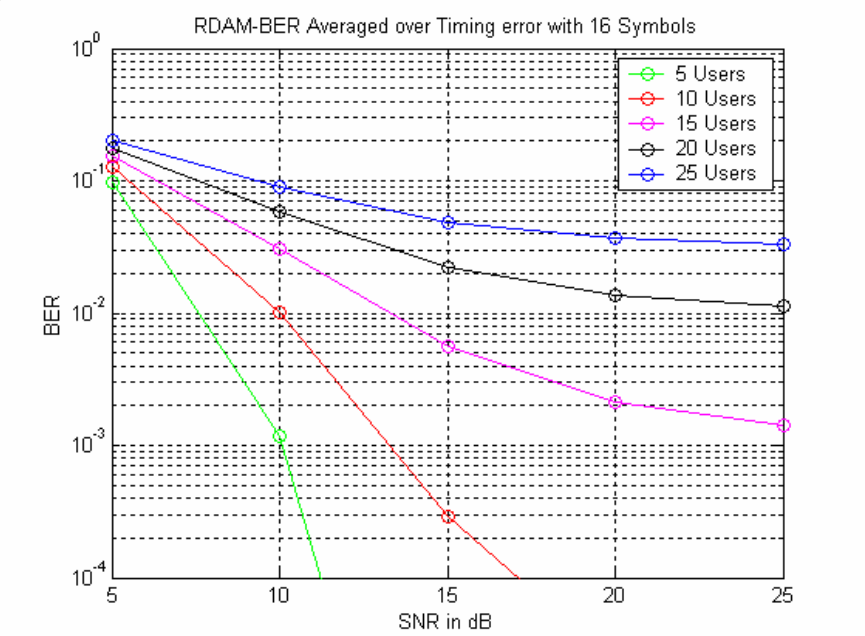

Figure 5.9: BER vs SNR for Increasing N_u, with M=16 Symbols

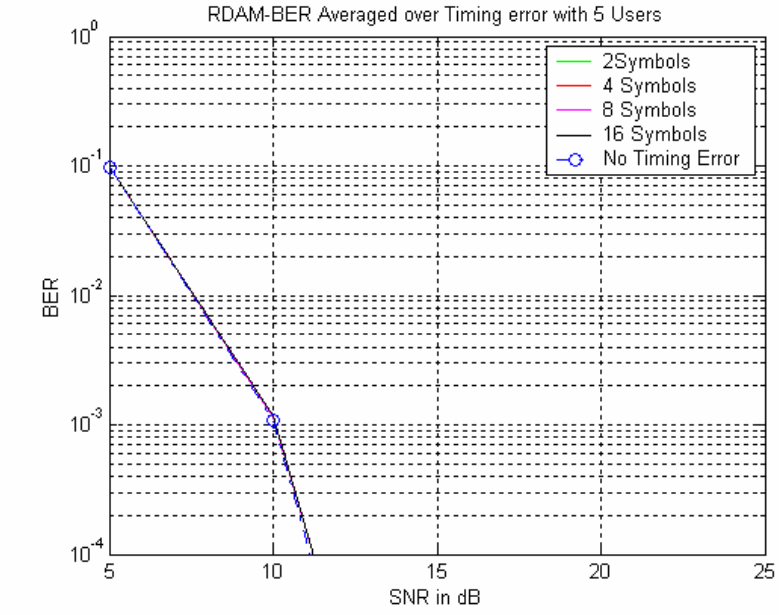

Figure 5.10: BER vs SNR for Increasing M, with N_u=5 Users

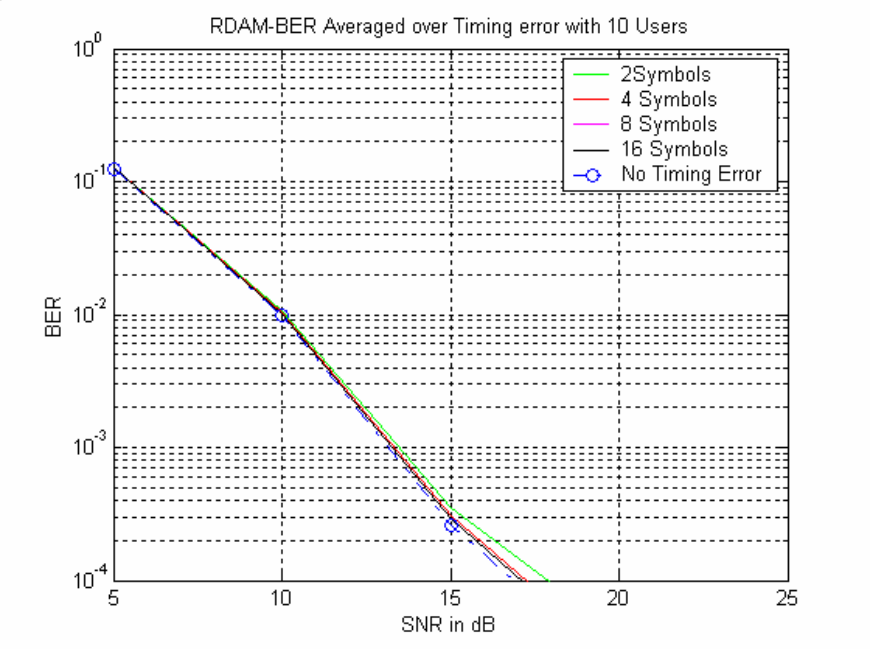

Figure 5.11: BER vs SNR for Increasing M, with N_u=10 Users

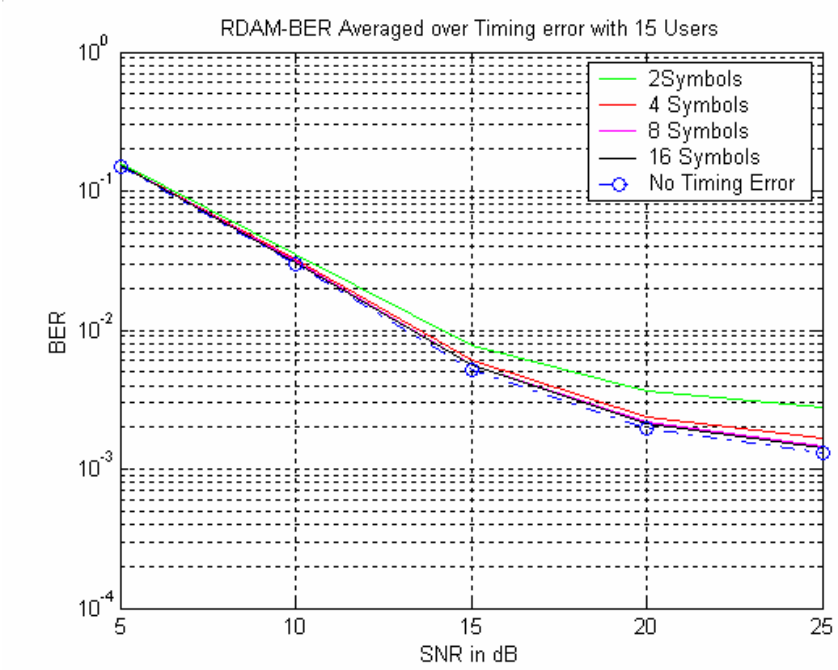

Figure 5.12: BER vs SNR for Increasing M, with N_u=15 Users

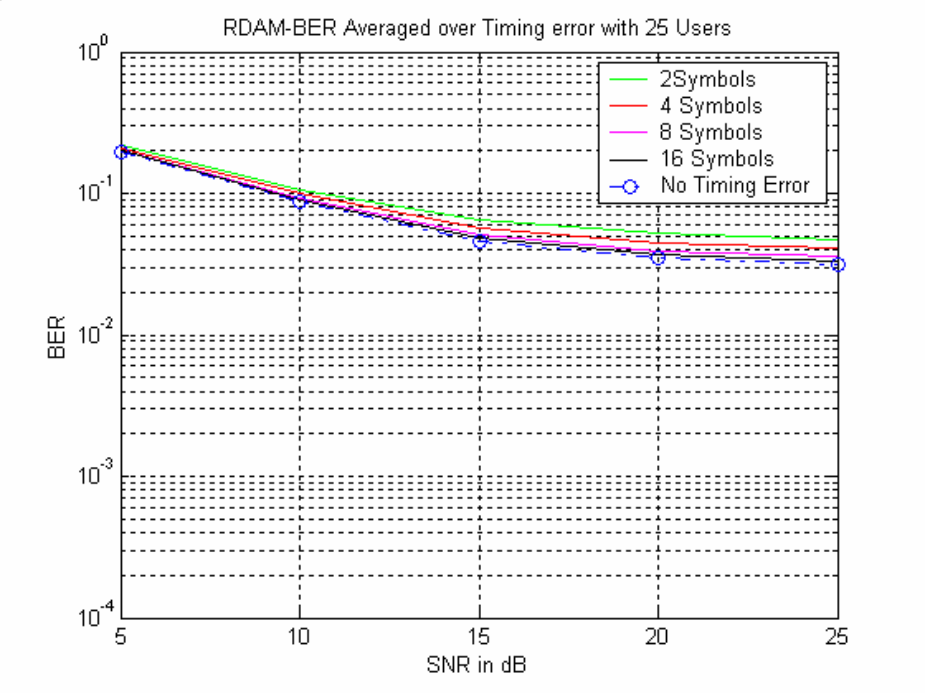

Figure 5.13: BER vs SNR for Increasing M, with N_u=25 Users

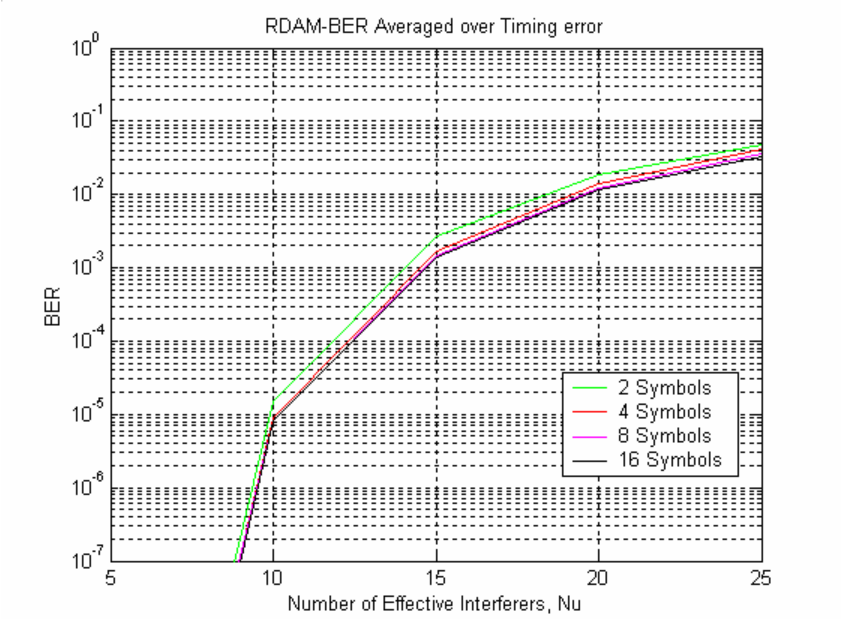

Figure 5.14: BER vs N_u for increasing M

In addition, the effect of N_u on BER performance for fixed M can be easily inferred from Figure 5.14. The performance improvements obtained with M=8 or M=16 are not significant, in terms

of BER, even though the difference is greatly perceivable in terms of the timing error performance. .

5.6 Results for an Ideal Rake Receiver

In the previous section, it was seen that in a differential detection receiver using ABS scheme for timing recovery, the effective number of users that can be tolerated is determined by the detection stage rather than the timing recovery stage. To compare with differential detection, we obtained the BER expressions for an ideal Rake receiver analytically and averaged them using the timing error PDFs from previous chapters. The coherent receiver uses a signal template to correlate with received signal, which is corrupted by multipath and multi-user interference as well as thermal noise. In this case, since the signal template is locally generated and noise-free, the resulting product has energy only at places where the template has a time-hopped pulse and zero energy everywhere else. In that case, the BER of the ideal Rake receiver in the presence of a timing error *n* can be give as:

$$BER_{nRAKE} = \frac{1}{2} Q\left[\sqrt{\frac{(N_c N_f - 2n)}{\left(N_u + \frac{N_c}{snr}\right)}}\right] + \frac{1}{2} Q\left[\sqrt{\frac{(N_c N_f)}{\left(N_u + \frac{N_c}{snr}\right)}}\right]$$

Thus, the effect of N_u on BER is greatly reduced as compared to differential detection. We averaged the BER_{nRake} with the PDF of timing error, for various values of M, SNR and N_u.

The use of the ABS scheme with ideal Rake reception has been tested with a spreading factor of 240, the timing error distributions being scaled versions of the timing error results obtained for differential detection. In addition, since there is less averaging when the spreading factor is 240, the scaled version is optimistic, similar to the assumption of perfect Rake reception. Thus, the results to be shown are upper bounds on Rake reception from the timing as well as detection aspects. Figures 5.15 and 5.16 illustrate the effect of timing acquisition error on the BER performance when a coherent Rake receiver is used. The effect of M is prominent from

Figure 5.15, with N_u=10 users. As M is increased from 2 to 32, the BER performance of the receiver tends to get close to the no-timing error case. With higher values of M, BER can almost match the values for perfect timing. Thus, the degradations due to timing errors can be compensated for, by using the ABS scheme with M>32.

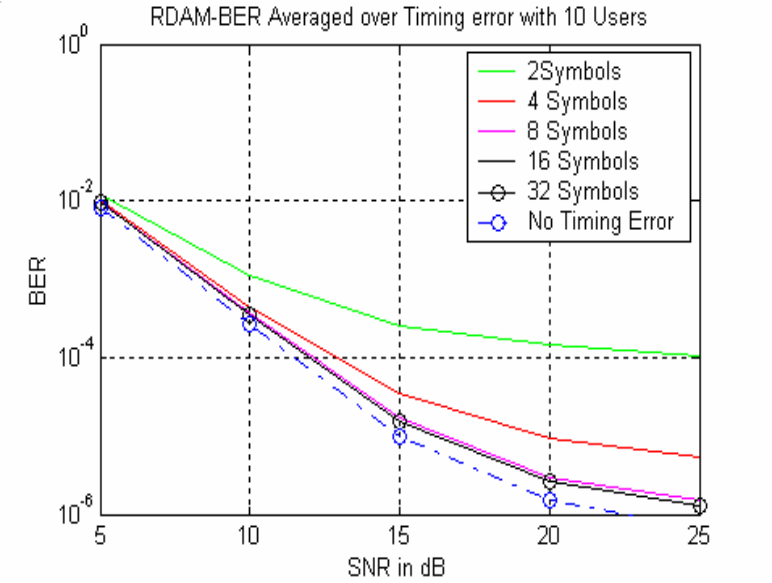

Figure 5.15: BER vs SNR for an ideal Rake Receiver, N_u=10 users

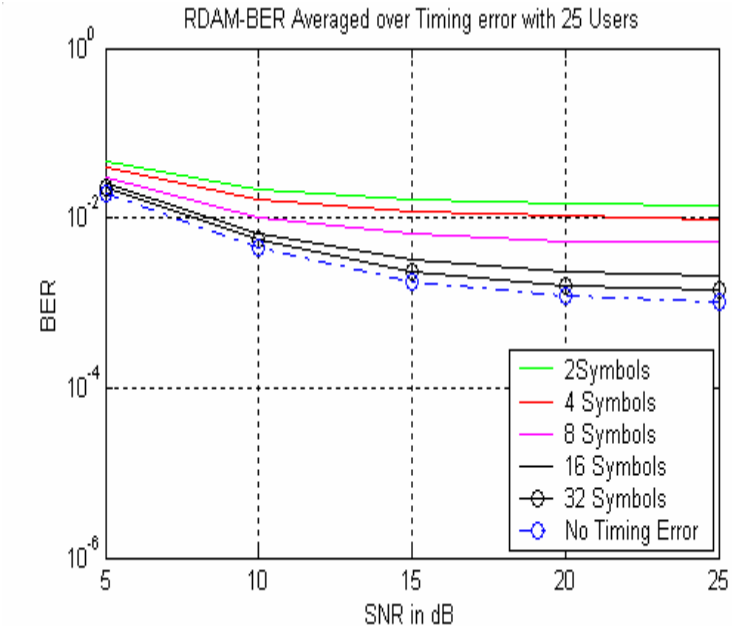

Figure 5.16: BER vs SNR for an ideal Rake Receiver, N_u=25 users

By contrast, observe from Figure 5.16 that, when N_u increases to 25, the effective number of users starts dominating the detection stage and even the use M=16 symbols for acquisition does not achieve BER performance close to the perfect timing case. In that case, degradations in the detection performance due to timing acquisition are discernible even with M=32. So, owing to the use of ABS scheme, timing acquisition gains significant with the use of an ideal Rake receiver, but not with differential detection. Greater improvements can be achieved with ABS scheme with the ideal Rake reception.

5.7 Additional Results

The use of differential detectors is advantageous in the ways that most of the received signal energy in multipath components can be captured due to self-Raking as previously described. But the self-Raking process leads to terms due to multiplication of interfering pulses and thermal noise components in each chip. Thus self-Raking has the effect of reducing the rate-per-bandwidth ratio of the receiver for high SNR scenarios. As shown in Appendix A.1, the rate-bandwidth-ratios can be calculated for both Rake and differential detectors as a function of the number of effective users in the system. Figure 5.17 shows the comparison of the rate-bandwidth-ratios for Rake and differential detectors as a function of number of users at high SNR values with perfect timing acquisition, for a BER value of 10^{-2}. Observe that the Rake receiver offers significant improvements over differential detectors for any number of users in the system. The effective transmitted rate reduces, for both receivers, as the number of effective interferers increases.

As a comparison to Figure 5.14, the effect of N_u on the BER performance of the Rake receiver is shown in Figure 5.18. The effect of increasing M to values of 16 and 32 is obvious in this case, with more improvements than in the case of differential detection.

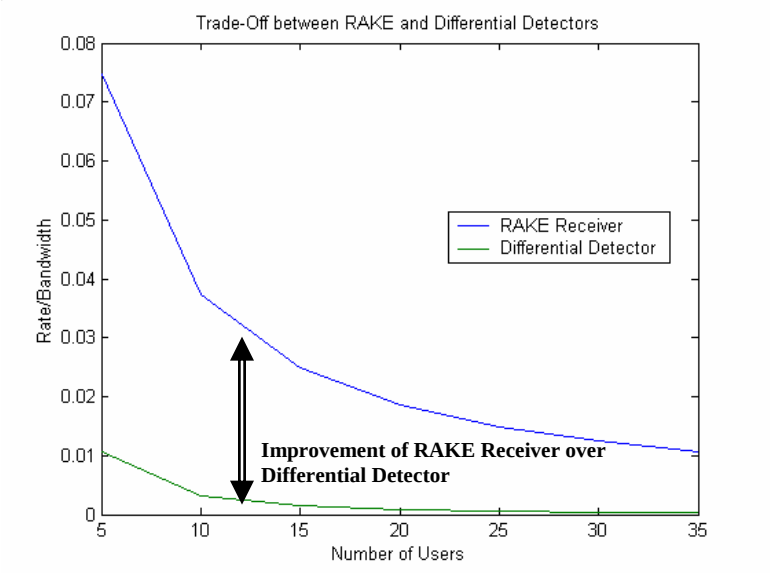

Figure 5.17: Rate-Bandwidth Ratio (R_b/W) vs N_u comparison for fixed BER (10^{-2}) (SNR~∞ with perfect timing acquisition)

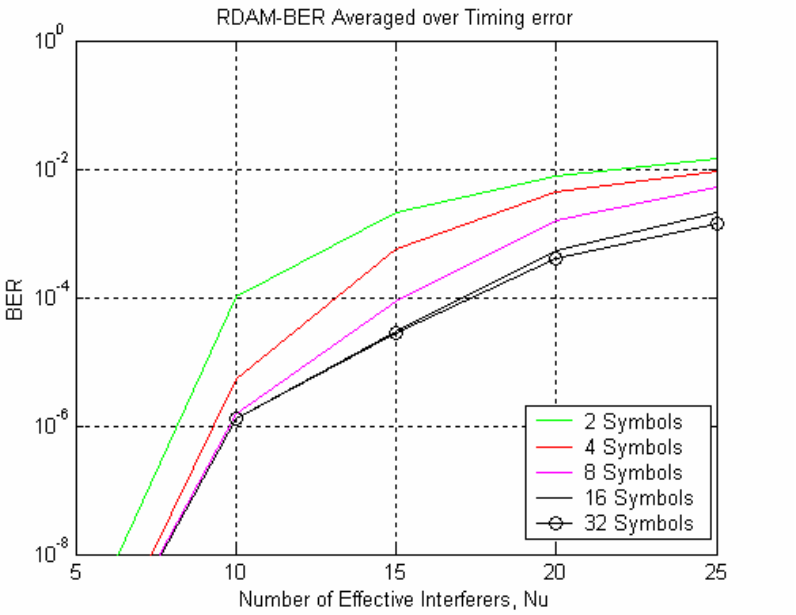

Figure 5.18: BER vs N_u for SNR=25dB, Rake receiver

Chapter 6

Summary and Conclusions

6.1 Summary

This thesis has analyzed the multi-user capabilities of the ABS scheme for IR based UWB systems. We illustrated the significance of the time hopping code pattern and its effect on the timing error statistics. Using the best TH pattern, the ABS scheme was applied in a multi-user scenario to evaluate the effect of M, SNR and N_u on the timing error distributions. Further, using a Gaussian approximation for multi-user and multi-path interference, we computed the theoretical bit error probabilities (BER) conditioned on the timing error, and then averaged the conditional BER using the simulation results of timing error probability density functions. BER performances have been compared for the differential detector and the ideal Rake receiver, both in conjunction with ABS timing.

The following is the outline of the important results:

- The statistics of absolute timing error are dependent on the TH pattern chosen. On comparing 4 different TH code patterns (USTH, RSTH, RDTH and RDAM TH schemes), it is to be noted that the RDAM TH pattern provides the lowest standard deviation of timing error. This happens because the amplitude modulation in the frames minimizes the random peak amplitude of pulses when interfering signals add up.
- The cumulative distribution functions of the absolute timing error are dependent on N_u, SNR and M. We show that for a fixed SNR and M, the timing error worsens as the value of N_u is increased. Thus, under low SNR conditions, with minimal number of symbols used for acquisition (say M=2), the performance of the ABS scheme is poor, i.e., since there is a high probability of huge timing errors. The timing performance of the scheme improves at higher SNR and for larger values of M. We showed that as the value of M increases, the

probability of higher timing error reduces greatly, even at low SNR and high interference conditions. It must also be noted that at higher M, acquisition speeds are reduced due to averaging over higher number of symbols. Thus there is a trade off between good timing and acquisition speed. With M=16, the timing errors can be reduced to be reduced to 4 frames, at high SNR, even with 25 users in the system. The number of users, N_u dominates over SNR and timing error as a limiting factor.

- As shown also in [41], the ABS scheme was shown here to perform better than other existing blind TDT algorithms [39, 40]. Thus the proposed ABS scheme can be used with MUI and multi-path, and will still perform better than the other algorithms in terms of system accuracy and acquisition speeds.
- Further, the BER performance of the differential detector in a multi-user multi-path environment has been analyzed. The BER performance degrades with increase in N_u, since the SINR is inversely related to N_u^2. Degradations in BER caused by the timing error are minor when the ABS scheme is implemented for timing recovery. For M=8 and M=16, the detection errors caused due to incorrect timing can be reduced significantly and BER performance close to the no-timing case can be achieved. Thus with ABS timing, the BER performance of a differential detector is less affected by timing error if $M \geq 8$.
- As a comparison to differential detection, the BER performance of the ideal Rake receiver has been analyzed, with the ABS scheme used for timing acquisition. It was observed that the timing error performance plays a critical role in the Rake detection. The effect of interference on the detection performance becomes prominent for higher values of N_u, but increasing M offers discernible improvements even with N_u=25 users. With higher values of M, a BER performance close to the no timing case can be attained. In order to accommodate more than 25 effective users, M>16 must be used; using M=32 provides adequate reduction of timing error impact. Thus, the use of the ABS scheme gains significance in a Rake receiver as compared to the differential detector.

- In addition to these results, we have also illustrated through simulations that the total multi-user interference power in each chip can be modeled as a Gaussian process. This assumption gains credence from the addition of multi-path components in a dense multi-path environment.
- With few changes at the transmitting end, modifications have been suggested to the current differential detector structures to prevent interference energy from being self-Raked at the receiver. Thus, we can tap the gains from self-Raking only for the desired user and keep the noise and interference floor to a minimum by avoiding self-Raking of interfering pulses.
- The use of differential detection definitely reduces the effective bit-rate of the system at high SNR and interference conditions, since the receiver performance is limited by the square of the number of effective interferers. There is a trade-off between receiver cost and complexity and effective transmitted bit-rate that deserves further study.

6.2 Benefits of the ABS Scheme

In a broadcast networks with varying number of nodes attaching and detaching from the network at a particular time, the ABS scheme plays an important role since it does not require a training sequence for the timing acquisition. The use of the ABS scheme in multi-user multipath environments provides us with distinct advantages:

- As the scheme is blind and differential in each symbol, the synchronization phase of the receiver is composed of simple delays and correlators. This greatly reduces cost and complexity of the receiver.
- The benefit of self-Raking is achieved even at the timing synchronization stage, capturing almost all the energy lost in multipath components, since the multipath profiles of the two half-symbol long windows used for correlation are alike.

- Superior timing error performance can be achieved and the impact of the timing errors on the BER performance of the receiver can be reduced by increasing M up to 16 and beyond. Even though this improvement comes with a reduction in acquisition speeds, we can infer from results in [41] that even with higher values of M, the algorithm offers faster synchronization compared to existing schemes.
- Dynamic variation of M is possible depending on the different interference and noise conditions. The potential of the communication link can be improved by dynamically increasing M according to the interference level (i.e *effective* number of interferers).
- BER performance close to the no-timing error case can be achieved by using the ABS scheme with values of M>8, with $N_u \leq 20$ users. This is true for both differential and Rake detectors.

Appendix A

A.1 Comparison of Rake Receiver with Differential Detector

The SINR for the case of no timing error for the Differential detector is already derived from Equation 5.6.At very high SNR values (>25 dB), this expression in Equation 5.6 can be approximated as

$$SINR_{no\_timing\_error} = \frac{N_f N_c}{\left(2(Nu) + (Nu)^2\right)}$$

Say for a BER of 10^{-2}, the required SINR is $SINR_0$, thus,

$$SINR_0 = \frac{N_f N_c}{\left(2(Nu) + (Nu)^2\right)} \text{ (or) } N_f N_c = \frac{1}{\left(2(Nu) + (Nu)^2\right) SINR_0}$$

Defining the rate-bandwidth-ratio R_b/W as $1/N_c N_f$,

$$\frac{Rb}{W}(diff) = \frac{1}{\left(2(Nu) + (Nu)^2\right) SINR_0}$$

For the Rake receiver, a signal template s'(t) is used to correlate with the received noisy signal s(t)+n'(t). Here we assume n'(t) is the Gaussian sum of interference and thermal noise.

The output of the correlator is

$$r(t) = (s(t) + n'(t)) * s(t) = s(t) * s(t) + n(t) * s(t)$$

At the output of the low pass filter,

$$\Im(t) = \int r'(t)\,dt = \int (s^2(t)dt + n'(t)s(t))dt$$

Using Parseval's theorem for Fourier transforms,

$$SINR_0 = \frac{[\int S(f)df]^2}{N_0[\int S(f)df]} = \frac{[\int S(f)df]}{N_0} = \frac{[\int S(f)df]}{\frac{P_{max}{}^2 . N_u}{N_c N_f}} = \frac{N_c N_f}{N_u}$$

Thus for the Rake receiver,

$$\frac{Rb}{W}(rake) = \frac{1}{(N_u) SINR_0}$$

where $\frac{Rb}{W}(rake) = \frac{1}{N_c N_f}$, $N_0 = \frac{P_{max}{}^2 . N_u}{N_c N_f}$ is the effective interference power in each chip (high SNR), and $P_{max}{}^2 = \int S(f)df = \int s^2(t)dt$]

A.2 Justification of transmit pulse shapes used for simulations

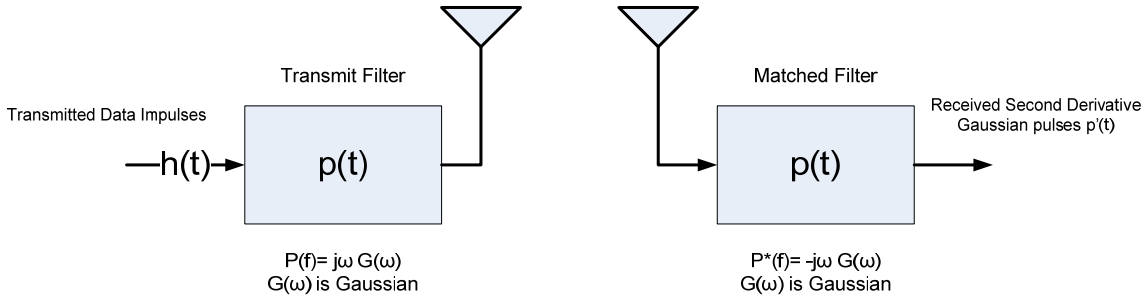

Consider a train of transmitted data impulses sent through a transmit pulse shaping filter with a Gaussian shaped frequency response. Let the spectrum of the transmit pulse p(t) after the transmit filter be represented by P(f)=jωG(ω). At the receiving end, the received signal is processed with a matched filter with impulse response -jωG(ω). The pulse at the output of matched filter has a spectrum of P(f)*P*(f) = $\omega^2 G^2(\omega)$, a second derivative of a Gaussian variable. $G^2(\omega)$ again is Gaussian since it is the product of two Gaussian variables. Let's call the resulting pulse as p'(t).

One frame of the received signal (for both differential timing acquisition as well as data detection) is considered. For simplicity, let's assume perfect synchronization is achieved at the receiver. The output of the integrator is

$$v_0(t) = \int_0^{T_f} (s(t) + n_1(t))(s(t) + n_2(t))dt$$

Where s(t) = p'(t) = P_{max}*h(t)

h(t) is a normalized second derivative of any pulse p(t) such that h(0)=1 and h(t≠ $\pm\tau_c$)=0. The signal power can be calculated as

$$P_{ss} = \int_0^{T_f} s^2(t)dt = \left[P^2{}_{\max} \int_0^{T_f} h^2(t)dt \right]^2 = P^4{}_{\max} \left[\int_0^{T_f} h^2(t)dt \right]^2$$

The noise components of $v_0(t)$ can be calculated as

$$v_{nn}(t) = \int_0^{T_f} n_1(t).n_2(t)dt$$

Thus the noise variance is,

$$P_{nn}= \overline{|v_{nn}(t)|^2} = \int_0^{T_f}\int_0^{T_f} \overline{n_1(t).n_1(t').n_2(t).n_2(t')}\; dtdt'$$

i.e, $$\overline{|v_{nn}(t)|^2} = \int_0^{T_f}\int_0^{T_f} \overline{n_1(t).n_1(t')}\;.\;\overline{n_2(t).n_2(t')}\; dtdt'$$

$$= \int_0^{T_f}\int_0^{T_f} \overline{n_1(t).n_1(t')}\;.\;\overline{n_2(t).n_2(t')}\; dtdt'$$

$$= \int_0^{T_f} R_{nn}(t)R_{nn}(t')dtdt' \;= T_f \int_0^{T_f} {R_{nn}}^2(t)dt'$$

To compute $R_{nn}(t)$, we need to define $n(t)$.

We know that in each frame, the noise term consists of all the pulses from other users corresponding to that frame as well as the multi-path components in that frame, or in any frame,

$$n(t) = \sum_i p(t - t_i)'$$

where i is the sum of the number of interfering pulses and multi-path components present in the frame.

Calculating $R_{nn}(t)$ as,

$$R_{nn}(t) = \int_0^{T_f} n(\tau).n(t-\tau)d\tau = \int_0^{T_f} \sum_i p(\tau - t_i)\sum_i p(t-\tau-t_i)'d\tau = \int_0^{T_f} \frac{T_f {P_{\max}}^4 {N_u}^2}{{N_c}^2} h^4(t)dt$$

The ratio $\frac{P_{ss}}{P_{nn}}$ gives us,

$$\frac{P_{ss}}{P_{nn}} = \frac{N_c\left[\int_0^{T_f} h^2(t)\right]^2}{{N_u}^2\left[\int_0^{T_f} h^4(t)dt\right]} \text{ where the ratio } \frac{\left[\int_0^{Tf} h^2(t)\right]^2}{\left[\int_0^{Tf} h^4(t)dt\right]} = T_c \approx 1ns(assumed)$$

Similarly, the ratio can be calculated for cross term between signal and interference terms. The pulse shape is defined by $h(t)$ and any pulse with the ratio above close to 1 *ns* is a good approximation for simulations. For a second derivative of Gaussian mono pulse, the value of this ratio was calculated to be approximately 1.17.

References

[1] L. Yang and G. B. Giannakis. Ultra-wideband communications: an idea whose time has come. In IEEE Signal Processing Magazine, pages 26–54, Nov 2004.

[2] G. Aiello and G. Rogeson. Ultra-wideband wireless systems. In IEEE Microwave Magazine, pages 36–47, June 2003.

[3] M. Win and R. Scholtz. Impulse radio: how it works. In IEEE Communications Letters, pages 36 – 38, Feb 1998.

[4] M. Win and R. Scholtz. On the robustness of ultra-wide bandwidth signals in dense multipath environments. In IEEE Communication Letters, pages 51–53, Feb 1998.

[5] M. Win and R. Scholtz. Ultra-wide bandwidth time-hopping spread spectrum impulse radio for wireless multiple-access communications. In IEEE Transactions on Communications, pages 679–689, April 2000.

[6] FCC. First Report and Order: In the matter of Revision of part 15 of the Commission's Rules regarding Ultra-Wideband transmission systems. Technical report, FCC, April 2002.

[7] N. Boubaker and K. Letaief. Ultra wideband DSSS for multiple access communications using antipodal signaling. In IEEE International Conference on Communications, pages 2197–2201, May 2003.

[8] B. Sadler and A. Swami. On the performance of UWB and DS-spread spectrum communication systems. In IEEE Conference on Ultra Wideband Systems and Technologies, pages 289–292, May 2002.

[9] J. Foerster. The performance of a direct-sequence spread ultrawideband system in the presence of multipath, narrowband interference, and multiuser interference. In IEEE Conference on Ultra Wideband Systems and Technologies, pages 87–91, May 2002.

[10] L. Qinghua and L. Rusch. Multiuser receivers for DS-CDMA UWB. In IEEE Conference on Ultra Wideband Systems and Technologies, pages 163 – 167, May 2002.

[11] N. Boubaker and K. Letaief. Ultra wideband DSSS for multiple access communications using antipodal signaling. In IEEE International Conference on Communications, pages 2197–2201, May 2003.

[12] B. Vojcic and R. Pickholtz. Direct-sequence code division multiple access for ultra-wide bandwidth impulse radio. In IEEE Military Communications Conference, pages 898–902, Oct 2003.

[13] P. Runkle, J. McCorkle, T. Miller, and M. Welborn. DS-CDMA: the modulation technology of choice for UWB communications. In IEEE Conference on Ultra Wideband Systems and Technologies, pages 364–368, Nov. 2003.

[14] V. S. Somayazulu, “Multiple access performance in UWB systems using time hopping vs. direct sequence spreading,” IEEE Wireless Communications and Networking Con− ference, Vol. 2, pp. 522-525, March 2002.

[15] A. Molisch, J. Foerster, and M. Pendergrass. Channel models for ultrawideband Personal Area Networks. In IEEE Wireless Communications, pages 14–21, Dec. 2003.

[16] A. Saleh and R. Valenzuela. A statistical model for indoor multipath propagation. In IEEE Journal on Selected Areas in Communication, pages 128–137, 1987.

[17] V. Lottici, A. Andrea, and U. Mengali. Channel estimation for ultra-wideband communications. In IEEE Journal on Selected Areas in Communication, pages 1638–1645, 2002.

[18] R. Hoctor and H. Tomlinson. Delay-hopped transmitted reference RF communications. In IEEE Conference on Ultra Wideband Systems and Technologies, pages 265–270, 2002.

[19] L. Yang and G. Giannakis. Optimal pilot waveform assisted modulation for ultrawideband communications. In IEEE Transactions on Wireless Communications, pages 1236–1249, 2004.

[20] H. Zhang and D. Goeckel. Generalized transmitted-reference UWB systems. In IEEE Conference on Ultra-Wideband Systems and Technologies, pages 147–151, Nov. 2003.

[21] G. Lu, P. Spasojevic, and L. Greenstein. Antenna and pulse designs for meeting UWB spectrum density requirements. In IEEE Conference of Ultra-wideband systems and technologies, pages 162–166, Nov. 2003.

[22] Z. Luo, H. Gao, Y. Liu, and J. Gao. A new UWB pulse design method for narrowband interference suppression. In IEEE Global Telecommunications Conference, pages 3488– 3492, Dec. 2004.

[23] E. Homier and R. Scholtz. Rapid acquisition of ultra-wideband signals in the dense multipath channel. In IEEE Conference on Ultrawideband systems and technologies, May 2002.

[24] J. Oh, S. Yang, and Y. Shin. A rapid acquisition scheme for UWB signals in indoor wireless channels. In Wireless Communications and Networking Conference, pages 1143– 1147, March 2004.

[25] M. Win and R. Scholtz. On the energy capture of ultra-wide bandwidth signals in dense multipath environments. In IEEE Communication Letters, pages 245–247, Sep 1998.

[26] S. Vijayakumaran and T. Wong. Equal gain combining for acquisition of UWB signals. In IEEE Miltiary Communications Conference, pages 880–885, October 2003.

[27] R. Fleming, C. Kushner, G. Roberts, and U. Nandiwala. Rapid Acquisition for ultrawideband localizers. In IEEE Conference on Ultra Wideband Systems and Technologies,
pages 245–249, May 2002.

[28] J. Furukawa, Y. Sanada, and T. Kuroda. Novel initial acquisition scheme for impulse based UWB systems. In IEEE Conference on Ultra Wideband Systems and Technologies, pages 278–282, May 2004.

[29] L. Reggiani and G. Maggio. A reduced complexity acquisition algorithm for UWB impulse radio. In IEEE Conference on Ultra wideband Systems and Technologies, pages 131–135, Nov. 2003.

[30] L. Reggiani and G. Maggio. Rapid search algorithms for code acquisition in UWB impulse radio communications. In IEEE Journal on Selected Areas in Communications,
pages 898–908, May 2005.

[31] Z. Tian and V. Lottici. Efficient timing acquisition in dense multipath for UWB signals. In IEEE Vehicular Technology Conference, pages 1318–1322, Oct. 2003.

[32] Z. Zhang and L. Ge. Differential detection acquisition for time-hopping sequence in ultrawideband radio. In 14th International Symposium on Personal, Indoor and Mobile Radio Communication, pages 2442–2445, 2003.

[33] Z. Zhang, L. Ge, B. Chen, and C. Li. Differential detection acquisition in multiple access time-hopping ultra-wideband communications. In International Workshop on Ultra-wideband systems, pages 283–287, May 2004.

[34] S. Aedudodla, S. Vijayakumaran, and T. Wong. Rapid ultra-wideband signal acquisition. In Wireless Communications and Networking Conference, pages 1148–1153, March 2004.

[35] U. Mengali and U. Mitra. Synchronization and channel estimation for UWB signals. In IEEE Global Telecommunications Conference, pages 764–768, Dec. 2003.

[36] L. Yang, Z. Tian, and G. Giannakis. Non-data aided timing acquisition of ultra-wideband transmissions using cyclostationarity. In IEEE International Conference on Acoustics, Speech and Signal Processing, pages 121–124, April 2003.

[37] Z. Tian, L.Wu, and S. Zekavat. Blind v/s training-based UWB timing acquisition with effective multipath capture. In The Thirty Seventh Asilomar Conference on Signals, Systems and Computers, pages 1771–1775, Nov. 2003.

[38] L. Yang and G. Giannakis. Low complexity training for rapid timing acquisition in ultra wideband communications. In IEEE Global Telecommunications Conference, pages 769– 773, Dec. 2003.

[39] L. Yang; Giannakis, G.B, Timing ultra-wideband signals with dirty templates in Volume 53, Issue 11, Nov. 2005 Page(s):1952 – 1963

[40] L. Yang and G. Giannakis. Blind UWB timing using a dirty template. In IEEE International Conference on Acoustics, Speech and Signal Processing, pages 509–512, May 2004.

[41] Shishir Agrawal, *A Novel Algorithm for Blind acquisition of ultra wideband signals*, MS Thesis, Rutgers University, May 2005.

[42] Minnie Ho, V.Srinivasa Somayazulu, Jeffery Foerster and Sumit Roy, A Differential Detector for an UWB Communication systems, IEEE Vehicular Technology Conf., vol. 4, no. 9, pp. 1896 - 1900, May. 2002.

[43] F. Ramirez-Mireles, “On Performance of Ultra Wideband Signals in Gaussian Noise and Dense Multipath,” IEEE Trans. Vehic. Tech., Vol. 50, Issue 1, Jan. 2001.

[44] J. Foerster, “The Effects of Multipath Interference on the Performance of UWB Systems in an Indoor Wireless Channel,” Proceedings of VTC2001, May 2001.

[45] L. Zhao, A. Haimovich, and H. Grebel, “Performance of Ultra-Wideband Communications in the Presence of Interference,” Proc. IEEE Int. Conf. On Comm., 2001.